Developmental and Comparative Immunology 129 (2022) 104339

Contents lists available at ScienceDirect

Developmental and Comparative Immunology

journal homepage: www.elsevier.com/locate/devcompimm

Perkinsus marinus suppresses *in vitro* eastern oyster apoptosis via IAP-dependent and caspase-independent pathways involving TNFR, NF-kB, and oxidative pathway crosstalk

Erin M. Witkop [a], Gary H. Wikfors [b], Dina A. Proestou [c], Kathryn Markey Lundgren [c], Mary Sullivan [c], Marta Gomez-Chiarri [a,*]

[a] University of Rhode Island, Department of Fisheries, Animal and Veterinary Science, 120 Flagg Rd, Kingston, RI, USA
[b] NOAA Northeast Fisheries Science Center Milford Laboratory, 212 Rogers Ave, Milford, CT, USA
[c] USDA ARS NEA NCWMAC Shellfish Genetics Program, 120 Flagg Rd, Kingston, RI, USA

ARTICLE INFO

Keywords:
Apoptosis
Oyster
Differential expression
IAP
WGCNA
Dermo disease

ABSTRACT

The protozoan parasite *Perkinsus marinus* causes Dermo disease in eastern oysters, *Crassostrea virginica*, and can suppress apoptosis of infected hemocytes using incompletely understood mechanisms. This study challenged hemocytes *in vitro* with *P. marinus* for 1 h in the presence or absence of caspase inhibitor Z-VAD-FMK or Inhibitor of Apoptosis protein (IAP) inhibitor GDC-0152. Hemocytes exposure to *P. marinus* significantly reduced granulocyte apoptosis, and pre-incubation with Z-VAD-FMK did not affect *P. marinus*-induced apoptosis suppression. Hemocyte pre-incubation with GDC-0152 prior to *P. marinus* challenge further reduced apoptosis of granulocytes with engulfed parasite, but not mitochondrial permeabilization. This suggests *P. marinus*-induced apoptosis suppression may be caspase-independent, affect an IAP-involved pathway, and occur downstream of mitochondrial permeabilization. *P. marinus* challenge stimulated hemocyte differential expression of oxidation-reduction, TNFR, and NF-kB pathways. WGCNA analysis of *P. marinus* expression in response to hemocyte exposure revealed correlated protease, kinase, and hydrolase expression that could contribute to *P. marinus*-induced apoptosis suppression.

1. Introduction

Infection with the alveolate parasite *Perkinsus marinus*, the causative agent of Dermo disease, contributes to seasonal mortality and decline of the eastern oyster, *Crassostrea virginica*, along the Gulf of Mexico and Atlantic coasts of the United States (Smolowitz, 2013). *P. marinus* trophozoites potentially gain entry into the oyster host during filter feeding through parasite migration across mucosal interfaces and/or by engulfment by granulocytes, a type of hemocyte and the main phagocytic oyster immune cell (Allam et al., 2013; Lau et al., 2018a; Smolowitz, 2013; Vasta et al., 2020; Wikfors and Alix, 2014; Yadavalli et al., 2020). This process may be mediated by oyster lectins (Vasta and Wang, 2020). Complex host responses are induced in granulocytes following *P. marinus* engulfment, including release of cytotoxic enzymes, reactive oxygen species (ROS), and serine protease inhibitors by hemocytes (Anderson et al., 1992; He et al., 2012; La Peyre et al., 2010; Lau et al., 2018b; Sullivan and Proestou, 2021). *P. marinus* can overcome or suppress host hemocyte defenses, particularly respiratory burst and apoptosis (a form of regulated cell death) pathways, through release of serine proteases, such as perkinsin, or ROS-neutralizing enzymes, such as superoxide dismutase (SOD) (Anderson, 1999; Anderson et al., 1992; Faisal et al., 1999; Fernández-Robledo et al., 2008; Lau et al., 2018b). Inhibition of host ROS and apoptotic responses may prolong granulocyte survival, thereby allowing for increased *P. marinus* intracellular replication, leading to dissemination of infected parasites through tissues, and, eventually, hemocyte lysis and parasite release (Alavi et al., 2009; Anderson, 1999; Anderson et al., 1992; Smolowitz, 2013; Volety and Chu, 1995). Apoptosis of eastern oyster hemocytes, therefore, is a key immune response to *P. marinus*, and increased apoptosis of *P. marinus*-infected granulocytes may contribute to oyster disease resistance by disrupting a replicative intracellular niche (*i.e.* protected from oyster immune responses) for the parasite, thereby limiting the

; IAP, Inhibitor of Apoptosis Protein; WGCNA, Weighted Gene Co-expression Network Analysis.

* Corresponding author.
E-mail address: gomezchi@uri.edu (M. Gomez-Chiarri).

https://doi.org/10.1016/j.dci.2022.104339
Received 1 October 2021; Received in revised form 29 December 2021; Accepted 1 January 2022
Available online 5 January 2022

speed of parasite propagation and disease progression within tissues (Goedken et al., 2005a,b; Hughes et al., 2010). *P. marinus* suppression of oyster hemocyte apoptosis, however, is nuanced and variable according to factors such as such as *P. marinus* strain, salinity, level of host resistance, and time post-infection (Goedken et al., 2005a; Hughes et al., 2010; Lau et al., 2018b; Proestou and Sullivan, 2020; Yee et al., 2005). Oyster apoptotic responses to *P. marinus* and mechanisms of *P.* marinus-induced host apoptosis suppression remain incompletely described.

In bivalve molluscs, apoptosis is critical for maintaining cellular homeostasis and defenses against pathogens and parasites, and involves two separate but linked pathways (Gerdol et al., 2018; Kiss, 2010; Romero et al., 2015). The intrinsic, or mitochondrial, apoptosis pathway is stimulated by intrinsic damage (reactive oxygen species, UV radiation, etc.) and is characterized by mitochondrial outer membrane permeabilization (MOMP). In contrast, the extrinsic, or death receptor-mediated, apoptosis pathway is triggered by extrinsic binding of ligands to pattern-recognition receptors and does not typically involve MOMP. Both pathways converge on action of the caspase family of cysteine-aspartic proteases which cleave apoptosis substrates and lead to apoptosis execution (Galluzzi et al., 2016). Caspase-independent apoptosis pathways have been identified in bivalves and involve release of mitochondrial enzymes, such as Apoptosis Inducing Factor (AIF) and endonuclease G (endoG), which translocate to the nucleus and trigger the final steps of apoptosis (Romero et al., 2015).

Previous research suggests that *P. marinus* suppression of eastern oyster hemocyte apoptosis involves modulation of ROS and stimulation of the pro-survival Nuclear Factor-Kappa B (NF-kB) pathway (Hughes et al., 2010; Lau et al., 2018b), a mechanism of host apoptosis suppression identified in other intracellular parasite systems. Mechanisms of host apoptosis evasion or suppression by the intracellular parasite *Toxoplasma gondii*, for example, involve prevention of mitochondrial cytochrome *c* release, caspase enzyme inhibition, and activation of the NF-kB pathway involving complexes of TRAFs and BIRC2/3 (cIAP1/-cIAP2) (Lodoen and Lima, 2019; Sangaré et al., 2019a). *T. gondii* additionally triggers upregulation of antiapoptotic Bcl-2 family proteins and Inhibitor of Apoptosis (IAP) proteins (Mammari et al., 2019). The IAP, or Baculoviral IAP Repeat-Containing (BIRC) gene family, is a critical family of apoptosis regulatory genes involved in both the intrinsic and extrinsic apoptosis pathways which has been recently characterized in oysters (Estornes and Bertrand, 2015; Witkop et al., in press BMC Genomics). The oyster IAP gene family is highly diverse and expanded, and IAP expression is tightly associated with apoptosis pathway expression across diverse immune challenges, suggesting their potential involvement in apoptosis regulation (Witkop et al., in press BMC Genomics).

To further understand apoptosis mechanisms involved in oyster granulocyte response to *P. marinus*, this study performed *in vitro* hemocyte assays coupling flow cytometry and dual transcriptomics of *C. virginica* and *P. marinus*. Specifically, the role of caspases, MOMP, and IAPs in hemocyte *P. marinus* response were evaluated after hemocyte pretreatment with the IAP inhibitor GDC-0152 and the pan-caspase inhibitor Z-VAD-FMK (Ekert et al., 1999; Flygare et al., 2012). This research helps elucidate the role of apoptosis in eastern oyster host-parasite interactions and reveals specific hemocyte immune pathways and *P. marinus* apoptosis-modulatory enzymes for future investigation.

2. Materials and methods

2.1. Oyster source and maintenance

Eastern oysters were obtained from the family-based breeding program at the Aquaculture Genetics and Breeding Technology Center (ABC) at the Virginia Institute of Marine Science (VIMS). Oyster juveniles (<one year old, shell height 52–106 mm) from 22 selectively-bred families with varying levels of survival in the Chesapeake Bay were delivered to the USDA ARS Shellfish Genetics Laboratory, Kingston, RI, in early June 2020 and subjected to a state-required disinfection protocol. Oyster maintenance and parasite challenge protocols have been previously described in detail (Proestou et al., 2019). Briefly, oysters were maintained in a 750-L, recirculating, aerated aquarium system running 1-μM filtered, UV-sterilized seawater following filtration. Oysters were acclimated to experimental conditions of 25 °C and 25 PSU over a period of two weeks and fed daily with Shellfish Diet 1800® instant algae (Reed Mariculture) throughout the experiment. Temperature was maintained at 25 °C using tank heaters when necessary and kept at ambient salinity (25–30 PSU) until hemolymph extraction.

2.2. Perkinsus marinus culture

Perkinsus marinus from ATCC® strain 50508 (American Type Culture Collection), a strain comparable in virulence to *P. marinus* strains present in the Chesapeake Bay (Bushek and Allen, 1996), was used. Cultures were used during the more virulent, log-phase growth stage (Ford et al., 2002). Parasite cell preparation for challenge was performed according to previous protocols (Proestou and Sullivan, 2020). Briefly, *P. marinus* cells were concentrated in 50-mL falcon tubes by centrifugation at 1,500 g for 5 min at 4 °C and washed using 0.45-μM filtered, sterile seawater at 28 PSU (FSSW, Red Sea) three times. Cells were stained with neutral red, counted with a hemacytometer and light microscope, and cell count was adjusted to the desired stock concentration for treatment.

2.3. Hemolymph isolation and preparation

To assess general *in vitro* mechanisms of apoptotic response to *P. marinus* independent of the disease resistance level of each sampled oyster family, and to have sufficient hemocytes to perform multiple assays and treatments in parallel using the same samples, three biological replicate pools were prepared using hemolymph extracted from a mix of randomly-selected oysters from the 22 families (total of 48 mL in each of the 3 hemolymph pools, n = 48–60 oysters per hemocyte pool, 1–3 oysters per family per pool). Oysters were scrubbed and cleaned using a freshwater rinse, shells were notched using small, hand-held wire cutters prior to bleeding, and hemolymph was collected from each oyster through the notch using a using a sterile, 1.5″ 25 G needle and 1-mL syringe primed with 100 μL of ice-cold, 0.45-μM filtered sterile seawater (FSSW) (Hégaret et al., 2003a). As much hemolymph as possible (average of 0.5 mL per oyster) was collected from each oyster, filtered using a 75-μM mesh screen to remove large debris and tissue that may interfere with flow cytometry analysis and added to the respective hemolymph pool. Hemocyte concentrations in each pool were quantified using neutral red staining on a hemacytometer with a light microscope, and *P. marinus* volumes required to achieve the desired 1:1 Multiplicity Of Infection (MOI) were calculated based upon hemocyte concentrations in each pool. Hemolymph suspensions were stored on ice through all procedures to avoid hemocyte aggregation and used within hours of extraction from oysters. All assays were performed using undiluted hemolymph and the required amount of sample for each assay (viability, apoptosis, caspase 3/7, phagocytosis, and RNA-seq; as described below) was aliquoted out of each of the three pools and kept on ice until processing.

2.4. Dose and temporal effects of GDC-0152 and Z-VAD-FMK on oyster hemocytes

The effects of IAP inhibitor GDC-0152 (ApexBio Technology, cat. no A4224) and pan-caspase inhibitor Z-VAD-FMK (BD, CAT# BDB550377) on oyster hemocyte viability, apoptosis, and caspase 3/7 activity in the absence of *P. marinus* were determined using flow cytometry to identify proper doses and incubation times for these inhibitors and investigate basal mechanisms of hemocyte apoptosis (see methods below). This experiment was performed prior to the main experiment and utilized

oysters from a single family to minimize biological variability. Hemolymph pools (n = 2 pools per treatment, n = 8 oysters per pool) were incubated at room temperature with different concentrations for each inhibitor (10, 50, or 100 μM) or control (FSSW) for either 3 or 4 h. Each treatment was performed in duplicate.

2.5. In vitro challenge of oyster hemocytes with P. marinus for flow cytometry

Live *P. marinus* cells used for oyster hemocyte challenge were incubated with 2 μL of a 1-mM stock solution of CellTrace Far Red live cell stain (ThermoFisher C34564) in DMSO per 1 mL of *P. marinus* culture (final concentration 2 μM), to facilitate identification of these cells in downstream flow cytometry analysis. Cells were gently agitated following reagent addition and incubated for 30 min at room temperature in the dark. Following incubation, cells were centrifuged at 2,000 g for 10 min at 4 °C, supernatant was removed, and cells were resuspended in 1 mL FSSW, and counted using a hemocytometer to adjust concentration to the amount needed for 1:1 MOI.

Hemolymph (200 μL for the caspase 3/7 activity assay, 100 μL for all other assays) was aliquoted into sterile, 5-mL polystyrene, round-bottom tubes for flow cytometry to achieve a final concentration ranging between 5–9 × 10^3 cells per tube, depending upon the initial hemocyte concentration of each pool and the assay. Treatments, each performed in triplicate, included: 1) Negative Control: hemolymph and FSSW; 2) Positive Control: hemolymph plus fluorescent beads (~6 μM Flow Check Ruby Red microspheres, Polysciences, CAT # 24288-5) coated with the pathogen-associated molecular pattern LPS (ThermoFisher, CAT #00-4976-93) (1:1 hemocyte to beads ratio based upon starting hemolymph concentration); 3) *P. marinus*: hemolymph incubated with live-stained *P. marinus* at a 1:1 multiplicity of infection (MOI); 4) IAP inhibitor assay: hemolymph preincubated for 3 h with 50-μM of the IAP inhibitor GDC-0152 plus live-stained *P. marinus* at a 1:1 MOI; 5) Caspase inhibitor assay: hemolymph preincubated for 1 h with 100-μM Z-VAD-FMK plus live-stained *P. marinus* at a 1:1 MOI. Hemolymph samples were incubated with *P. marinus* (1:1 MOI based on initial hemolymph pool cell concentration), beads (1:1 MOI based on initial hemolymph pool cell concentration), or FSSW for 1 h at room temperature, and flow cytometry was performed as described below.

2.6. Flow cytometry

Four assays were performed using hemolymph from each of the biological replicate pools: a) viability assay (4 μL 10X SYBR Green – SYBR- or 4 μL of 1 mg/mL propidium iodide – PI - in 100 μL hemolymph and 300 μL FSSW) to measure the proportion of live (SYBR Green) and dead (PI) hemocytes in each sample (Croxton et al., 2012); b) apoptosis assay (FITC Annexin-V, BD Pharmingen, catalog # 556419; final concentration of 25 μL/mL in 100 μL hemolymph and 100 μL FSSW) to measure the proportion of apoptotic hemocytes in each sample (Hughes et al., 2010); c) caspase 3/7 activity (caspase) assay (CellEvent Caspase 3/7 Green Detection Reagent, Thermo Fisher, Cat #C10427; final concentration of 1.25 μL/mL in 200 μL hemolymph and 200 μL FSSW) to measure the proportion of caspase 3/7 active hemocytes in each sample; and d) mitochondrial outer membrane permeabilization (MOMP) assay to measure the proportion of hemocytes with permeabilized outer mitochondrial membranes, a critical morphological feature of intrinsic apoptosis (MitoProbe JC-1 Assay kit for Flow Cytometry, ThermoFisher Cat #M34152; 2 μM final concentration in 100 μL hemolymph and 100 μL FSSW (Rodriguez et al., 2020)). Following reagent addition, tubes in the caspase and viability assays were incubated for 1 h at room temperature in the dark, while apoptosis and MOMP assays incubated at room temperature in the dark for 15 min per manufacturer's instructions.

Additional control assays were performed for each biological replicate pool: 1) MOMP assay positive control, to confirm proper detection of MOMP in treated samples (hemolymph plus mitochondrial membrane disruptor CCCP; MitoProbe JC-1 Assay kit for Flow Cytometry, ThermoFisher Cat #M34152; 50 μM final concentration); 2) Unstained *P. marinus* control (for all 4 assays), to determine basal *P. marinus* parameters in the absence of oyster hemocytes (same amount of *P. marinus* cells as used to achieve a 1:1 MOI); 3) Fluorescent probe single stained compensation controls, in order to assist with proper gating during flow cytometry results analysis (SYBR Green plus hemolymph, PI plus hemolymph, CellTrace Far Red live cell stain plus *P. marinus*, fluorescent beads plus hemolymph); 4) Hemolymph phagocytosis assay (Hégaret et al., 2003b) to compare hemocyte rates of phagocytosis between beads vs. *P. marinus* (hemolymph plus LPS-coated beads, or hemolymph plus *P. marinus*).

Flow cytometry assays were run on a BD Accuri C6+ flow cytometer (BD) (NOAA NEFSC Milford Laboratory) for 1 min 30 s using a fast flow rate (66 μL/min) with a threshold of 100,000 on FSC-H. Instrument QC was checked prior to use with the BD CS&T RUO beads (Becton Dickinson, CAT # 661414). All flow cytometry plots were compensated using manufacturers recommendations in the BD Accuri C6 Plus flow Software (V 1.0.23.1). Populations of granulocytes and agranulocytes were gated using custom FSC-H vs SSC-H gates on scatterplots (Wikfors and Alix, 2014). Subpopulations of granulocytes positive for each assay, with and without engulfed *P. marinus*, were determined based upon custom quadrant gates (see "correction factor" procedure below). Gating single stained controls for each fluorescent probe and samples plotted as count histograms for each stain were utilized to precisely adjust gating positions for all assays.

Due to limitations in the number of available flow cytometer lasers (and, therefore, the number of simultaneously measurable fluorophores in each assay), and the fact that free *P. marinus* cells sometimes overlap with hemocytes in flow cytometry scatterplots due to their similar size and complexity, the specific contributions of free and hemocyte-engulfed *P. marinus* to the granular cell apoptosis, MOMP, and caspase 3/7 activity assay results was calculated indirectly by combining the following data: a) assay values (apoptosis, caspase 3/7, and MOMP phenotypes) for the unstained *P. marinus*-only controls (Supplementary Fig. 1); b) the combined total number of measured hemocytes and stained *P. marinus* in each sample; c) the total stained *P. marinus* cells measured in each sample; d) the average percent of *P. marinus* cells that overlap in size with granular hemocytes; and e) data derived from the phagocytosis assay, which identified the average percentage of phagocytosed *P. marinus* (Supplementary Fig. 1); These five values were used to calculate a "correction factor" for each assay that estimated the likely number of phagocytosed, granular hemocyte-overlapping, assay-positive free *P. marinus* present in the targeted gated quadrant. The value of this correction factor was then subtracted from the values for each assay in these relevant flow cytometry quadrants. This process is described in detail in the analysis code on github (Supplementary Figs. 1 and 3).

2.7. Flow cytometry statistical analysis

Results are expressed as average ± standard deviation (sd) of percent cells showing a particular phenotype (*i.e.* viability, apoptosis, etc.). Significant differences between treatment groups for apoptosis, viability, MOMP, and caspase 3/7 activity were measured using one-way and two-way ANOVA with arcsine-transformed cell percentage data to ensure normal distribution. Post-hoc testing was performed for ANOVA tests with the Tukey Honestly Significant Difference (HSD) test. For comparison of granular and agranular cell composition and viability between cell types, differences were assessed using a Student's T-test (*t. test*). All statistical analyses were performed in R Studio (V 3.6.1) (R Studio Team, 2020). Plots were generated in R Studio using *ggplot2* and compiled with *egg* (V 0.4.5) and *cowplot* (V 1.0.0) (see code on github).

2.8. Hemocyte in vitro challenge with P. marinus for transcriptome sequencing

Assays for transcriptome analysis were performed in parallel with the flow cytometry assays, using cells from the same hemolymph pools and the same experimental conditions, except for volume and the absence of fluorescent stains. Hemolymph pools were aliquoted into three sterile, 50-mL falcon tubes for each treatment (10 mL hemolymph each sample with 4.5–9 x 10^5 total hemocytes in each sample, 12 samples total, n = 3 for each treatment). The following treatments were performed: 1) Hemolymph only; 2) Hemolymph plus unstained *P. marinus* (MOI 1:1); 3) Hemolymph pretreated for 3 h with the IAP inhibitor GDC-0152 plus *P. marinus* (MOI 1:1); 4) Hemolymph pretreated for 1 h with the pan-caspase inhibitor Z-VAD-FMK plus *P. marinus* (MOI 1:1). All treatments were incubated for 1 h after *P. marinus* addition, at which point samples were centrifuged at 1,500×*g*, 4 °C for 15 min, supernatant was removed, cell pellets were flash frozen in liquid nitrogen, and samples were stored at −80 °C prior to RNA extraction.

2.9. RNA extraction, cDNA synthesis, sequencing

Cell pellets (from 10 mL hemolymph) were lysed by incubation with 750 μL of Trizol reagent (Invitrogen, CAT# 15596018) for 15 min on ice (ThermoFisher CAT #15596026). Cellular debris was removed by centrifugation at 12,000 g for 10 min at 4 °C. RNA was extracted with 200 μL of chloroform, shaken vigorously, and incubated at room temperature for 15 min. Following centrifugation at 12,000 at 4 °C for 15 min, the aqueous layer was removed. An additional chloroform extraction was performed with 500 μL of chloroform, shaken vigorously, and incubated at room temperature for 15 min. Following centrifugation at 12,000 g at 4 °C for 15 min, the aqueous layer was removed. RNase-free glycogen (5 μg; ThermoFisher, CAT #AM9510) was added to all samples as a carrier to the aqueous phase. Room temperature 500 μL of isopropanol was added and incubated for 10 min at room temperature, followed by centrifugation at 12,000×*g* for 10 min at 4 °C. Three sequential washes were performed with ice-cold, molecular grade 75% ethanol. Samples were air-dried for 5 min and resuspended in 15 μL of DEPC-treated water. Samples were DNase treated using the DNA-free DNA Removal Kit (Invitrogen, CAT #AM1906) using manufacturer recommendations. Quality and quantity of extracted RNA was assessed using the Nanodrop 8000 Spectrophotometer (ThermoFisher). cDNA library preparation and paired-end sequencing were performed by GENEWIZ (https://www.genewiz.com, Azenta Life Sciences, New Jersey, USA). An rRNA removal protocol was used during library prep and libraries were sequenced on Illumina Hi-Seq 2 x150bp at a depth of 15–20 million reads per sample.

2.10. Mapping and assembly of RNAseq data

BBTools BBMap (V 37.36) was used to trim adapters, quality trim the left and right sides of reads with Phred quality scores of less than 20 and remove entire reads with an average *Phred* score of less than 10 (Bushnell, 2014) (NCBI BioProject PRJNA769054). Transcriptomes were first aligned to the *C. virginica* reference genome sequence (GCF_002022765.2) using HISAT2 (V 2.1.0) with default parameters and without use of a reference annotation to allow for novel transcript discovery (Kim et al., 2016; Pertea et al., 2016). HISAT2 output files were sorted and converted to BAM format using SAMtools (V 1.9.0) (Li et al., 2009). Transcripts were assembled and quantified using the *C. virginica* reference genome annotation (GCF_002022765.2_C_virginica-3.0_genomic.gff) using Stringtie (V 2.1.0) (Pertea et al., 2016). Comparison of transcriptome annotation to the reference for each sample was conducted using *gffcompare* (V 0.11.5) (Pertea et al., 2016). Stringtie output was formatted into matrices of transcript count data and uploaded into R Studio (V 3.6.1) (R Studio Team, 2020). The same process for alignment, assembly, and quantification was repeated with transcriptome files using the *P. marinus* reference genome sequence and reference annotation (GCA_000006405.1). Scripts used for analysis are available on github.

2.11. Differential expression analysis

Differential expression of transcripts in both *C. virginica* and *P. marinus* RNAseq datasets was calculated using DESeq2 (V 1.24.0) in R Studio (V 3.6.1) (Love et al., 2014; R Studio Team, 2020). To analyze hemocyte differential gene expression, the formula "~condition" was used to compare each individual treatment to control non-treated hemocytes in a pairwise manner and results of individual comparisons were analyzed using the results() function. To analyze the effect of hemocyte inhibitor treatment on *P. marinus* differential gene expression, the formula "~condition" was used to compare *P. marinus* expression in *P. marinus* exposed to hemocytes alone with gene expression in *P. marinus* exposed to hemocytes pretreated with either GDC-0152 or ZVAD-FMK. Transcript counts were log-scale transformed and normalized to the library size using the *rlog* formula (Love et al., 2014). Transcripts with <10 counts were removed from analysis. Log fold changes (LFC) in expression between transcripts within experiments were considered significant when *p*-values adjusted (*Padj*) using the Benjamini–Hochberg to control for the False Discovery rate (FDR) were ≤0.05. LFC shrinkage was performed using "*apeglm*" to improve ranking transcripts by effect size and to enable comparison of LFC between experiments (Zhu et al., 2018). LFC heatmaps were generated with *ComplexHeatmap* (V 2.0.0) (Gu et al., 2016), transcript count heatmaps were produced with *pheatmap* (V) and volcano plots were generated with *ggplot2*. Gene Ontology enrichment was conducted with the list of significantly correlated genes in each module using the package *topGO* (V 2.36.0) (Alexa and Rahnenfuhrer, 2019) in R (V 3.6.1). GO terms for each protein were obtained by running the full protein sequences for the eastern oyster genome assembly (GCA_002022765.4) and the *P. marinus* assembly (GCA_000006405.1) through Interproscan (V 5.44). Bubble plots of GO enrichment data were created with *ggplot2*. Treemap plots were generated with REVIGO using default parameters and the *treemap* package (V 2.4–2) in R (Supek et al., 2011).

2.12. Weighted gene correlation network analysis (WGCNA) and GO enrichment

WGCNA (V 1.68) was performed in R (V 3.6.1) with the hemocyte and *P. marinus* expression datasets separately. For both data sets, expression data were transformed as for the DESeq2 experiment using the *rlog* transformation prior to network construction. Networks were constructed as "*signed hybrid*" type with robust correlation performed using the bi-weight mid-correlation (corFunc = "*bicor*") (Langfelder and Horvath, 2008). A soft thresholding power of 7 produced the best fit to scale free topology and was selected to construct each network. For the hemocyte WGCNA analysis, significant and interesting modules were identified based on the following criteria: 1) Modules significantly correlated with challenge condition (Pearson's correlation, *cor* function; p-value ≤ 0.05); 2) Contain apoptosis-related transcripts (annotated from Witkop et al., in press BMC Genomics); 3) High ($r > 0.4$) and significant ($p < 0.05$) correlation between gene significance and module membership, indicating that highly connected genes in the module were also significant for the effect of *P. marinus* challenge of hemocytes; 4) Significant correlation with apoptosis phenotype (arcsine transformed percentages of hemocytes that had engulfed *P. marinus* cells and were apoptotic). For *P. marinus* WGCNA analysis, significant and interesting modules were identified by: 1) Significant correlation of modules with challenge condition (Pearson's correlation, *cor* function), p-value ≤ 0.05); 2) High ($r > 0.4$) and significant ($p < 0.05$) correlation between gene significance and module membership; and 3) Significant correlation with apoptosis phenotype (arcsine transformed percentages of

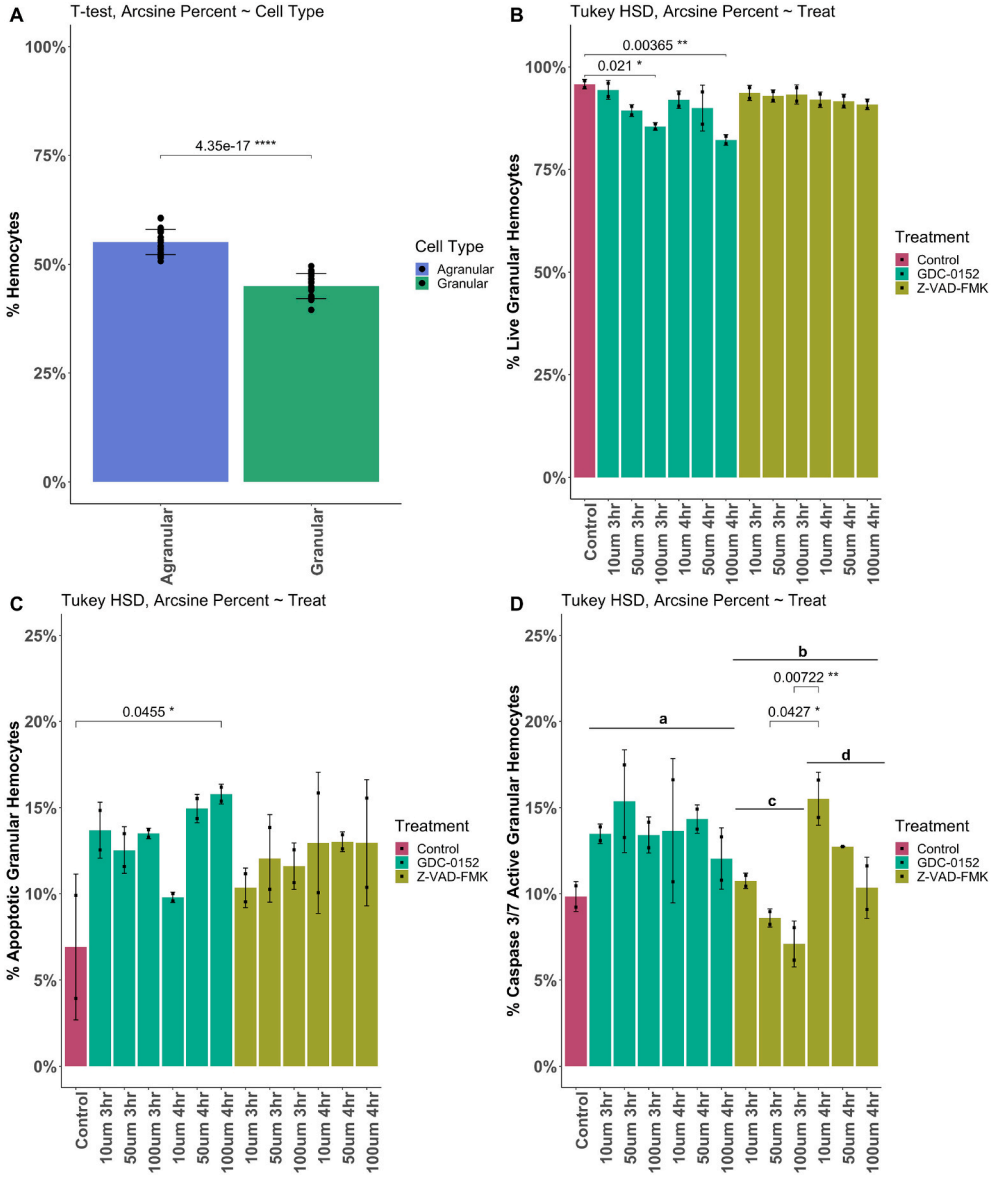

Fig. 1. Basal apoptosis in unstimulated granulocytes may be IAP-dependent and involve caspase-independent pathways. Percent (average±standard deviation, n = 3 hemolymph pools) of hemolymph composition (A) granulocyte viability (B), apoptosis (C), and caspase 3/7 activity (D) following treatment with either GDC-0152 or Z-VAD-FMK was measured by flow cytometry. (A) Percent of total (viable and unviable) granulocytes and agranulocytes in hemolymph (n = 3 pools). (B) Percent live granulocytes measured as 100% minus the percent PI stained. GDC-0152 (100 μM) significantly decreased granulocyte viability as compared to control. (C) Dose and time effect of inhibitor treatment on percent apoptotic granulocytes. GDC-0152 (100 μM, 4 h) significantly increased granulocyte apoptosis as compared to control. (D) Dose and time effect of inhibitor treatment on percent caspase 3/7 active granulocytes. No significant differences observed compared to control. GDC-0152 and Z-VAD-FMK treatments significantly differed from one another (One-Way ANOVA, $p = 0.004$, a vs. b), and the effect of time was significant in Z-VAD-FMK treatments (One-Way ANOVA, $p = 0.009$, c vs. d). Statistical tests were performed with arcsine transformed percentages (*$p <= 0.05$; **$p <= 0.01$; ***$p <= 0.001$). Significance is displayed only for treatments differing from control for (A) and (B).

hemocytes that had engulfed *P. marinus* cells and were apoptotic).

For both analyses, intramodular hub genes were identified as genes in each module with a high absolute value for gene significance (GS) > 0.6, and high absolute value for module membership (MM) (calculated with the *signedKME* function) > 0.8 (Langfelder et al., 2011; Liu et al., 2019). Gene Ontology enrichment was conducted with the list of significantly correlated genes in each module using the package topGO (V 2.36.0) (Alexa and Rahnenfuhrer, 2019) in R (V 3.6.1). Modules of interest (identified using criteria above) were exported from WGCNA using *exportNetworkToCytoscape* without prior subsetting for edge weight, and edge files were then uploaded to Cytoscape (V 3.8.0), along with corresponding product annotations and trait significance for visualization (Shannon et al., 2003). Selected modules were subset for apoptosis-related genes of interest (both hub genes and non-hub genes identified above in WGCNA based on GS for treatment and MM) and genes of interest with significant correlations with apoptosis phenotype. The network was drawn with the prefuse force directed layout using edge weight (Shannon et al., 2003). For *P. marinus* modules, nodes were filtered to keep intramodular hub genes for treatment and edges with weights greater than or equal to the 80th percentile of edge weights from the entire module. *P. marinus* modules were drawn using the circular layout.

3. Results

3.1. Basal apoptosis in unstimulated granulocytes may be IAP-dependent and involve caspase-independent pathways

Potential hemocyte apoptosis mechanisms and optimal conditions for treatment with inhibitors were investigated in unstimulated hemolymph (*i.e.* not challenged with *P. marinus*). Agranulocytes were more abundant on average than granulocytes in pooled hemolymph samples (55% ± 3% vs. 45% ± 3%, One-way ANOVA, Tukey HSD $p < 0.05$; Fig. 1a). Pan-caspase inhibitor Z-VAD-FMK treatment did not significantly affect granulocyte viability (as determined by membrane rupture) at any concentration (91–94% viable cells, $p > 0.5$), suggesting no cytotoxic effect (Fig. 1b). IAP inhibitor GDC-0152 treatment for 3 or 4 h significantly increased granulocyte cell death at the 100 μM dose only (One-way ANOVA, Tukey HSD, $p < 0.02$), indicating potential cytotoxicity at this concentration. To avoid potential cytotoxicity of GDC-0152, subsequent *in vitro* assays were performed with 3 h pre-incubation at a 50 μM final concentration.

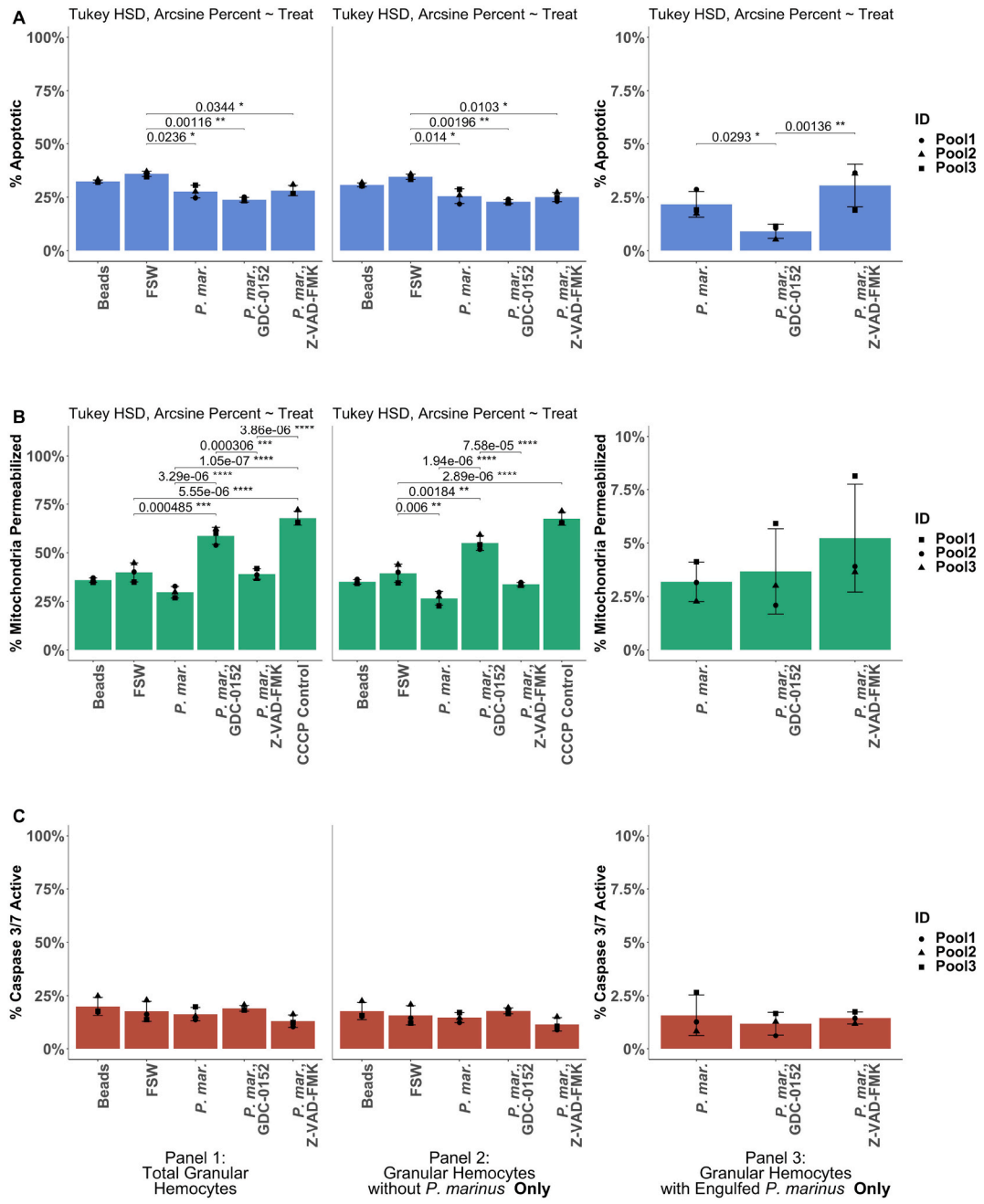

Fig. 2. Pretreatment with an IAP inhibitor affected *P. marinus* inhibition of apoptosis downstream of membrane permeabilization, while caspase inhibitors had no effect. Control and inhibitor-pretreated (IAP inhibitor GDC-0152 for 3 h or caspase inhibitor Z-VAD-FMK for 1 h) hemolymph was incubated for 1 h with activated beads or *P. marinus* at an MOI of 1:1, and the average±sd percent granular cell apoptosis (A, annexin-V assay), membrane permeabilization (B, JC-1 assay), and caspase 3/7 activation (C) was determined by flow cytometry. Percent of cells in different cellular portions (different gates) are presented: total granulocytes (left panel); granulocytes without engulfed *P. marinus* (middle panel), and granulocytes with engulfed *P. marinus* (right panel). Black lines represent the standard deviation. Statistical tests were performed with arcsine transformed percentages (*$p <= 0.05$; **$p <= 0.01$; ***$p <= 0.001$).

Overall, few unstimulated granulocytes and agranulocytes were apoptotic (Fig. 1c, Supplementary Fig. 2), although granulocyte apoptosis significantly differed in response to inhibitor treatment in the GDC-0152 treatment, but agranular cell apoptosis did not (Fig. 1c, Supplementary Fig. 2). Based upon this and the known importance of granulocytes in eastern oyster immune responses to *P. marinus* (La Peyre et al., 1995; Soudant et al., 2013; Vasta et al., 2020; Wikfors and Alix, 2014), granulocytes were the focus in subsequent analyses. As predicted by the demonstrated action of GDC-0152 in other organisms (Hu et al., 2015), IAP inhibition significantly increased granulocyte apoptosis compared to control (100 μM, 4 h, One-Way ANOVA, $p = 0.001$; Fig. 1c), revealing some or all granulocyte apoptosis may be IAP-dependent. Caspase 3/7 activation was not significantly affected by IAP inhibition in granulocytes (Fig. 1d), suggesting apoptosis triggered by IAP inhibition may be caspase-independent.

Treatment with pan-caspase inhibitor Z-VAD-FMK did not lead to a significant decrease in caspase 3/7 activation in hemocytes as compared to the already low levels seen in control samples (Fig. 1d). Despite no differences being observed between these treatments, lower levels of granulocyte caspase 3/7 activation were seen as the dose of the inhibitor increased, although this trend was also not significant (One-Way ANOVA, $p = 0.09$). However, levels of caspase 3/7 activation were

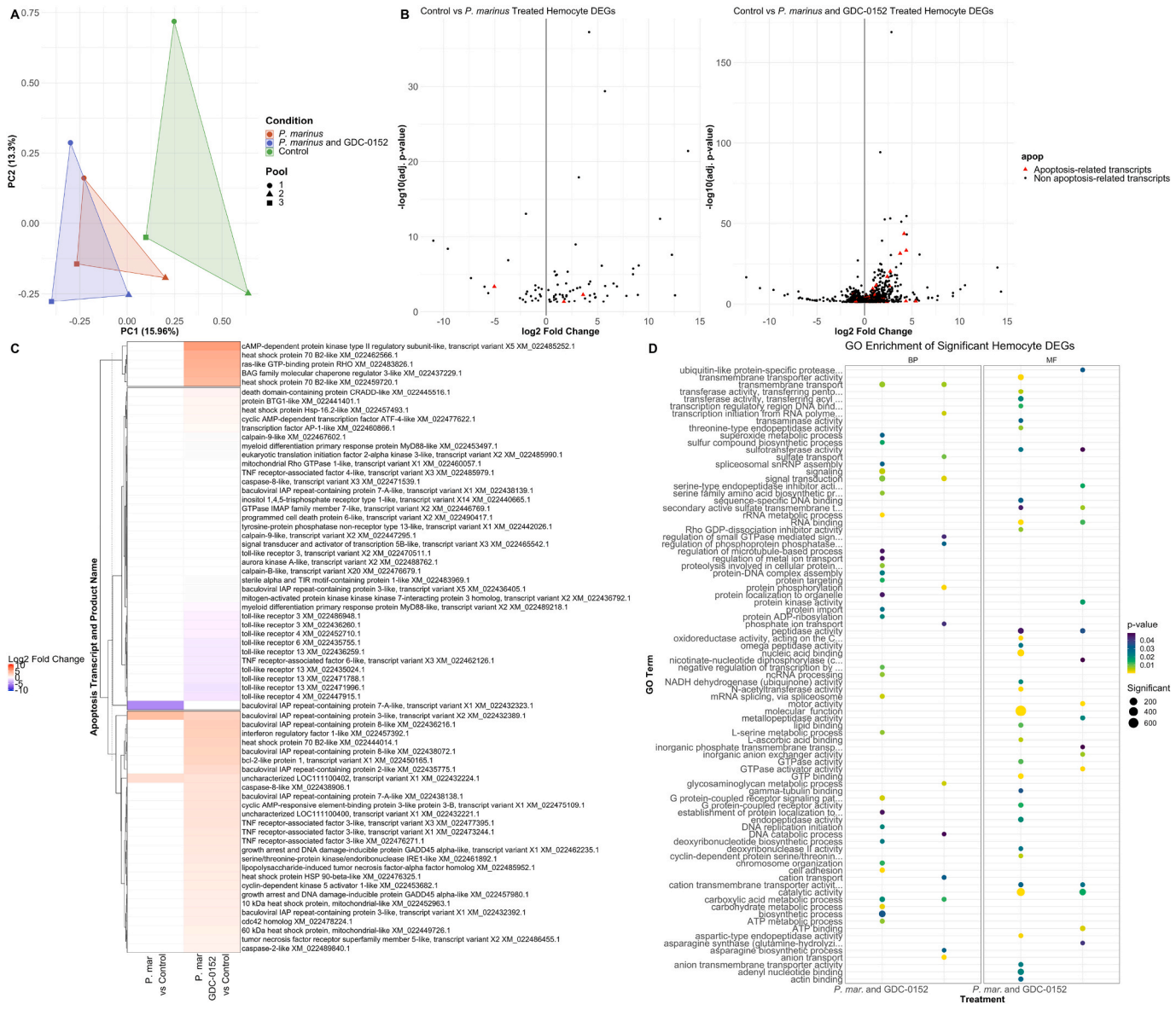

Fig. 3. Dual *P. marinus* and IAP inhibitor treatment triggered differential gene expression in oyster hemocytes of TNFR and NF-kB pathways and upregulation of oxidation-reduction processes. Hemocytes were pretreated with control (FSSW) or 50 μM of GDC-0152 for 3 h prior to incubation with *P. marinus* (1:1 MOI) for 1 h before processing for RNA extraction. Gene expression in each treatment was compared to control non-exposed hemocytes. (A) PCA plot of *rlog* transformed counts for each sample. (B) Volcano plots of DEGs, with those transcripts involved in apoptosis plotted with red triangles. Transcripts with negligible differential expression (−0.1-0.1) were excluded from plotting. (C) LFC plots of hemocyte apoptosis DEGs compared between both treatments. (D) Bubble plot showing significantly enriched BP and MF GO terms identified by topGO in each set of DEGs.

significantly lower at 3 h than 4 h post-exposure (One-Way ANOVA, $p = 0.009$, Fig. 1d), with caspase 3/7 activation significantly lower at 3 h than 4 h post-exposure, suggesting the slight effect of the inhibitor may have been transient, leading to a compensatory increase in caspase 3/7 after inhibition was released. Caspase 3/7 activation in Z-VAD-FMK treated hemocytes was also significantly lower overall than in GDC-0152 treatments (Fig. 1d, One Way ANOVA, Tukey HSD, $p = 0.02$). To streamline the assays (*i.e.* stagger the two inhibitor treatments) and measure results prior to any compensatory effects observed at longer incubation times, subsequent assays employed a 1 h hemocyte Z-VAD-FMK pretreatment at the highest tested dosage, 100 μM concentration.

3.2. Hemocyte IAP inhibitor pretreatment affected P. marinus apoptosis inhibition downstream of membrane permeabilization, but caspase inhibitor had no effect

Treatment with *P. marinus* significantly decreased granulocyte apoptosis compared to control in both subsets of hemocytes (containing and not containing engulfed *P. marinus*; $p < 0.02$; Fig. 2a, Supplementary Fig. 3a), confirming previous research showing that *P. marinus* suppresses hemocyte apoptosis (Goedken et al., 2005a; Hughes et al., 2010). Active phagocytosis of *P. marinus* by hemocytes was additionally confirmed (Supplementary Fig. 1a), also supporting previous research (Hughes et al., 2010), and *P. marinus* was phagocytosed at a significantly higher rate than LPS-activated beads (13% ± 2% of engulfed *P. marinus* vs 2% ± 1% of engulfed beads; One Way ANOVA, Tukey HSD $p = 0.0006$, Supplementary Fig. 1a). High viability of the *P. marinus* trophozoites utilized in all assays was shown with SYBR green staining

(95% ± 2% viable *P. marinus*, n = 3; Supplementary Fig. 1b).

To further investigate mechanisms of apoptosis inhibition by *P. marinus*, apoptotic activity was quantified after hemocytes were pretreated with the selective IAP inhibitor GDC-0152, which can affect both intrinsic and extrinsic apoptosis pathways (Erickson et al., 2013; Hu et al., 2015; Tchoghandjian et al., 2016). Although hemocyte pretreatment with GDC-0152 alone increased apoptosis in granulocytes compared to non-treated controls (Fig. 1c), pretreatment of hemocytes with GDC-0152 followed by *P. marinus* challenge led to a significant decrease in total granulocyte apoptosis (granulocytes with and without engulfed *P. marinus*; Fig. 2a, left panel) and apoptosis in granulocytes not containing engulfed *P. marinus* compared to control hemocytes (Fig. 2a, middle panel). Furthermore, apoptosis in granulocytes containing engulfed *P. marinus* was also significantly lower in the dual GDC-0152 and *P. marinus* treatment than in the treatment with *P. marinus* alone ($p = 0.03$, Fig. 2a). These results show that the effect of *P. marinus* on hemocyte apoptosis inhibition was even stronger when selected oyster IAPs are inhibited by GDC-0152, suggesting that normal *P. marinus* inhibition of granulocyte apoptosis is not directly mediated by the activity of GDC-0152-targetted IAPs, but could involve some interaction with IAP pathways.

Although total granulocyte apoptosis following GDC-0152 pretreatment and *P. marinus* challenge decreased compared to control (Fig. 2a, left panel), MOMP significantly increased ($p = 0.0005$; Fig. 2b, left panel, Supplementary Fig. 3b), an unexpected result because steps downstream of MOMP are expected to trigger apoptosis. Furthermore, in the granulocytes containing engulfed *P. marinus*, MOMP was not significantly affected by GDC-0152 pretreatment (Fig. 2b, right panel, Supplementary Figs. 3a and b), although dual GDC-0152 and *P. marinus* treatment led to significant apoptosis suppression (as compared to hemocytes challenged only with *P. marinus*; Fig. 2a, right panel). These results imply that *P. marinus* suppressed apoptosis downstream of MOMP.

Finally, *P. marinus* treatment, coupled with either Z-VAD-FMK or GDC-0152 treatment, had no significant effect on caspase 3/7 activity (Fig. 2c, Supplementary Fig. 3c), suggesting apoptotic processes suppressed by *P. marinus* do not involve caspase activation.

3.3. *P. marinus* triggered expression of oyster genes involved in catalytic and proteolytic activity, RNA binding, and metabolic processes in hemocytes, but few genes in apoptosis pathways

Differential gene expression of hemocytes challenged with *P. marinus* was first evaluated. Transcriptome sequencing produced 10–30 M reads per sample (not shown) and *rlog* transformed read counts clustered by hemocyte pool and treatment (Fig. 3a). *P. marinus*-challenged hemocytes differentially expressed 518 total transcripts compared to control untreated hemocytes, most of which were upregulated in response to *P. marinus* (Fig. 3b). Few apoptosis-related transcripts, 15 total and 3 with LFC >1, all of which were IAP transcripts, were differentially expressed in hemocytes challenged with *P. marinus* (Fig. 3b). Of the 3 differentially expressed IAP transcripts, two were upregulated (LFC >2, BIRC2/3-like, and TY-BIR-RING), and one was strongly downregulated (BIRC5-like, LFC = −5) (IAP annotations from Witkop et al., in press BMC Genomics). Differentially expressed apoptosis-related transcripts with low LFC (<1) included some involved in the TLR pathway (TLR13, MyD88, TRAF4), the TNFR pathway (BIRC2/3-like, caspase 8), and the ER and calcium signaling pathway (IP3R, PDCD6, calpain 9). These results show that *P. marinus* exposure triggered hemocyte expression of IAP proteins, but little change in apoptosis pathway gene expression overall.

Eighteen molecular function (MF) and 14 biological process (BP) GO terms were significantly enriched (Fisher's Exact test, $p \leq 0.05$) (Fig. 3d) in the differentially expressed hemocyte transcripts responding to *P. marinus*. The top five significant MF terms were protein binding (GO:0005515), motor activity (GO:0003774), GTPase activator activity (GO:0005096), and ATP binding (GO:0005524), and the top five significant BP terms were anion transport (GO:0006820), protein phosphorylation (GO:0006468), signal transduction (GO:0007165) and transcription initiation from RNA polymerase (GO:0006367). Additional enriched terms were associated with key enzymes involved in parasitic infection response (Chakraborti et al., 2019; Dean et al., 2014; Siqueira-Neto et al., 2018; Xue, 2019), including serine-type endopeptidase inhibitor activity (GO:0004867), protein kinase activity (GO:0004672), peptidase activity (GO:0008233), and metallopeptidase activity (GO:0008237). Serine protease inhibitors (serine-type endopeptidase inhibitor) are important *C. virginica* secreted enzymes in defense against *P. marinus* and other pathogens (Xue, 2019), and 3 transcripts were significantly differentially expressed with this GO term; two inter-alpha-trypsin inhibitor heavy chain H3-like proteins (XP_022300431.1, XP_022300432.1) possessing inter-alpha-trypsin domains (IPR013694), and one spondin-1-like transcript (XP_022294477.1) which possessed basic protease (Kunitz-type) inhibitor family signatures (IPR002223).

Finally, REVIGO analysis revealed RNA binding, catalytic activity, motor activity, protein binding, GTPase activator activity, and cation transmembrane transporter activity to be the most representative enriched GO molecular functions, and anion transport, glycosaminoglycan metabolic processes and regulation of small GTPase mediated signal transduction to be the most representative biological processes in *P. marinus* exposed hemocytes (Supplementary Figs. 4a and b).

3.4. Hemocyte pretreatment with IAP inhibitor GDC-0152 followed by *P. marinus* challenge led to upregulation of oxidation-reduction processes and modulation of TNFR and NF-kB pathway signaling

Differential expression analysis was also used to better understand mechanisms contributing to further apoptosis suppression in the dual GDC-0152 and *P. marinus* treatment (Fig. 3). This treatment stimulated three times as many differentially expressed transcripts compared to challenge with *P. marinus* alone (1577 versus 518) and included a higher number of transcripts associated with apoptosis-related pathways, with 62 differentially expressed transcripts (17 with LFC≥1 or ≤ −1) compared to 15 (Fig. 3b right panel, d, Supplementary Fig. 5). More GO terms were also significantly enriched (44 MF, 37 BP) compared to *P. marinus* treatment alone (Fig. 3d). The top five significant MF GO terms included protein binding (GO:0005515), ATP binding (GO:0005524), DNA-binding transcription factor activity (GO:0003700), unfolded protein binding (GO:0051082), and oxidoreductase activity, acting on diphenols and related substances as donors (GO:0016679). The top five BP enriched GO terms included protein folding (GO:0006457), oxidation-reduction process (GO:0055114), regulation of transcription, DNA-template (GO:0006355), tRNA aminoacylation for protein translation (GO:0006418), and tissue regeneration (GO:0042246). Additional enriched GO terms previously implicated in intracellular parasite infections (Chakraborti et al., 2019; Siqueira-Neto et al., 2018; Xue, 2019) were regulation of metal ion transport (GO:0010959), superoxide metabolic processes (GO:0006801), and several endopeptidase related terms, including peptidase activity, endopeptidase activity (GO:0004175), threonine-type endopeptidase activity (GO:0004298) and aspartic-type endopeptidase activity (GO:0004190) (Fig. 3d). REVIGO analysis of BP terms highlighted regulation of metal ion transport, metabolic processes, oxidation-reduction process, superoxide metabolic process and protein folding, among others, as key representative terms in the set of enriched BP terms (Supplementary Fig. 4d).

The enrichment of oxidation-reduction processes observed in hemocytes in response to dual GDC-0152 and *P. marinus* treatment was not observed with hemocyte *P. marinus* treatment alone, but has been identified previously as a key component of oyster response to *P. marinus* (Fernández-Robledo et al., 2008; Lau et al., 2018b; Schott et al., 2003; Sullivan and Proestou, 2021; Xue, 2019). DEGs representing enriched

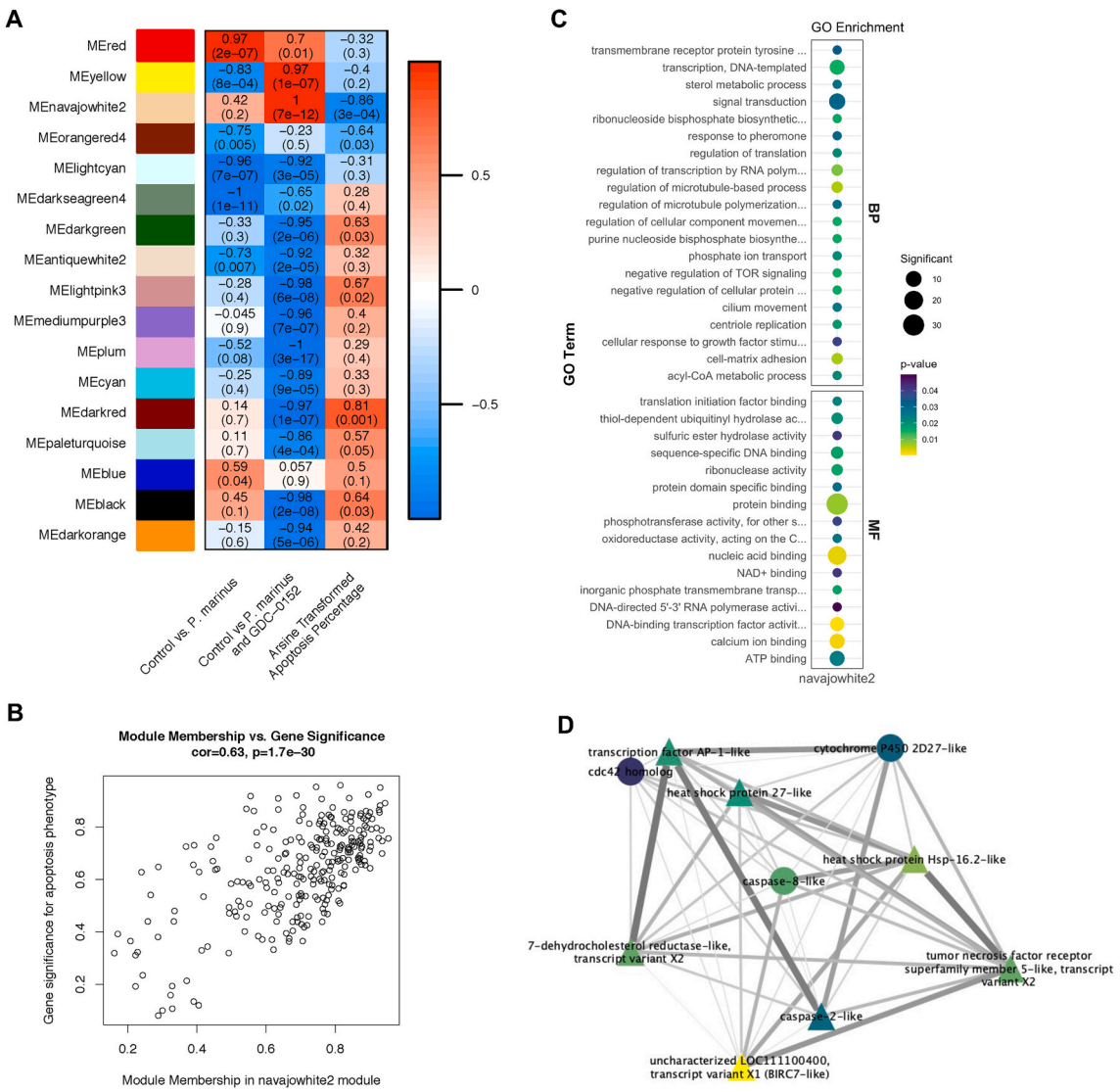

Fig. 4. TNFR pathway and oxidoreductase transcript expression in oyster hemocytes were significantly correlated with apoptosis transcripts and apoptosis phenotype following dual *P. marinus* and IAP inhibitor treatment. Hemocytes were pretreated with control (FSSW) or 50 μM of GDC-0152 for 3 h and then incubated with *P. marinus* (1:1 MOI) for 1 h before analysis of hemocyte gene expression. Associations between hemocyte gene expression and apoptosis phenotype (percent granular cell apoptosis in response to treatment) were investigated using WGCNA. (A) Heatmap of modules selected based on the following criteria: significantly correlated with either *P. marinus* challenge alone or GDC-0152 and *P. marinus* treatment, showing high Gene Significance (GS) and Module Membership (MM) relationship, and containing apoptosis intramodular hub genes. Modules are plotted with their correlation with apoptosis phenotype. X-axis indicates modules of correlated transcripts and the y-axis plots each trait for which module significance was calculated. Correlation values (-1 – 1), followed by and significance values (*p* between 0 and 1) in parentheses, are listed in each cell. Color indicates strength and direction of correlation. (B) Relationship between GS and MM for the navajowhite2 module, where each point is a transcript in the module. (C) GO enrichment for Biological Process (BP) and Molecular Function (MF) for the navajowhite2 module. (D) Hemocyte navajowhite2 module network (Cytoscape, V 3.8.0) showing apoptosis-related and oxidoreductase genes of interest significantly correlated with apoptosis phenotype. Nodes colored by significance for apoptosis phenotype (yellow = high significance, blue = low significance), edge width and color were scaled to edge weight (thicker = higher weight, darker = higher weight), and node shape indicated hub gene status (triangle = hub gene, circle = non-hub gene).

superoxide metabolic processes included superoxide dismutase [Cu-Zn], chloroplastic-like (XP_022304796.1) and glutenin, high molecular weight subunit DX5-like (XP_022314583.1) which contains a Cu-Zn-superoxide dismutase family signature. DEGs also contained oxidoreductase activity related transcripts, which included a conditioned medium factor receptor 1-like (XP_022336529.1) with a GG-red-SF: geranylgeranyl reductase family domain, and 7-dehydrocholesterol reductase-like transcripts (XP_022318313.1, XP_022318314.1).

Further investigation of significantly differentially expressed apoptosis-related transcripts in the dual GDC-0152 and *P. marinus* treatment revealed complex responses of multiple apoptotic pathways, including strong upregulation of intrinsic (mitochondrial apoptosis, oxidative stress, ER stress, DNA damage response) and extrinsic apoptosis pathways (TNFR pathway, NF-kB pathway), strong upregulation of multiple IAPs, and downregulation of the TLR pathway (Fig. 3c). Inflammatory pathways and extrinsic apoptosis were the most responsive apoptosis related pathways, including receptors (TNRSF5, TLR3,4,6,13), receptor adapter proteins (TRAF3,4,6, BIRC2/3-like), signal transduction molecules (MyD88), inhibitory molecules (hsp70, BAG3, hsp90), transcription factors (LITAF, AP-1, IRF1), and effector molecules (caspase 8, IRF1), although NF-kB specifically was not identified as differentially expressed. A total of 8 IAP transcripts were differentially expressed, 7 of those upregulated with LFC >1, including 2 BIRC2/3-like, 1 BIRC7-like, 1 novel BIRC11, 1 novel BIRC12, and two

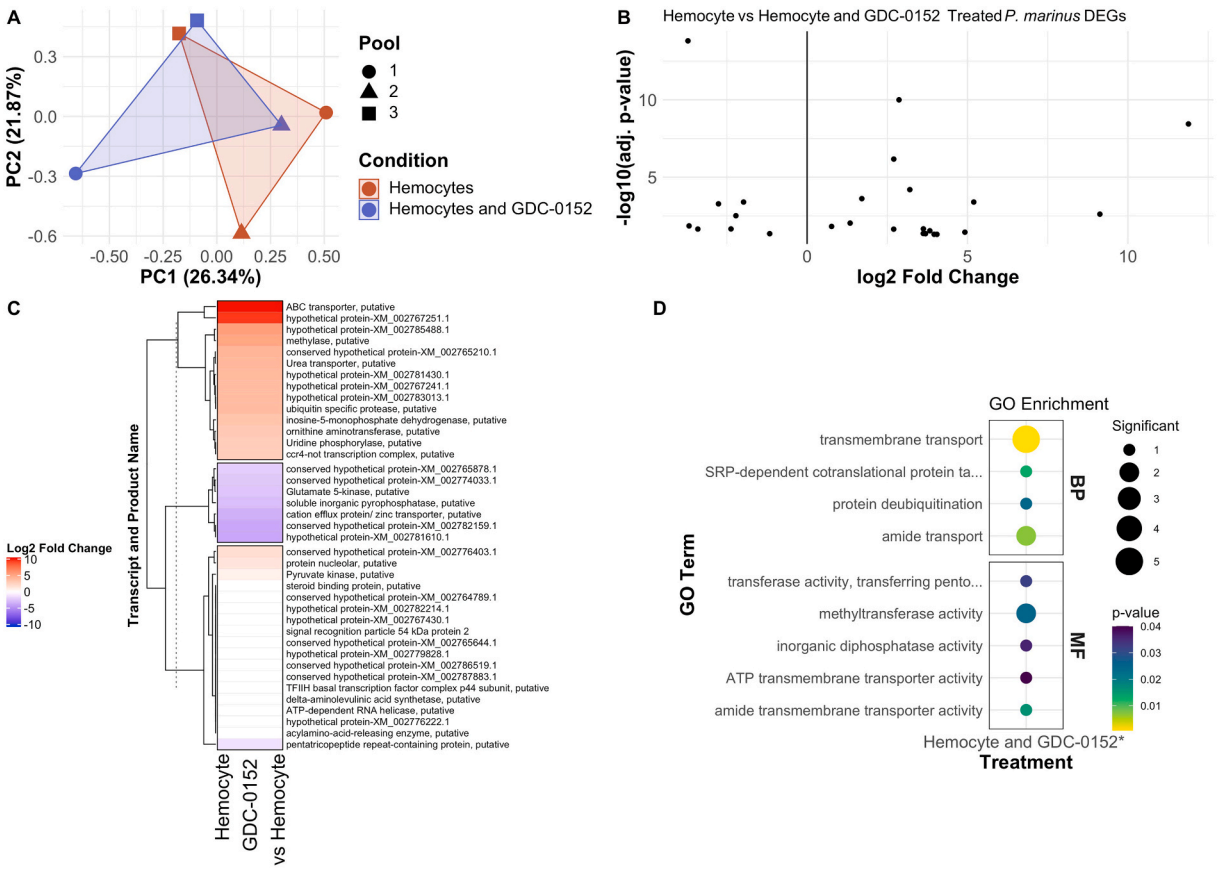

Fig. 5. Pre-exposure of hemocytes with GDC-0152 before treatment with *P. marinus* induced differential expression of transporter genes in *P. marinus*. Hemocytes were pretreated with control (FSSW) or 50 μM of GDC-0152 for 3 h and then incubated with *P. marinus* (1:1 MOI) for 1 h before analysis of *P. marinus* gene expression. *P. marinus* DEGs were analyzed in comparison to *P. marinus* expression in control (non-GDC treated) hemocytes. (A) PCA plot of *rlog* transformed counts for each sample. (B) Volcano plots of differentially expressed genes (DEGs) in *P. marinus* in response to GDC-0152 pretreatment of hemocytes. Transcripts with negligible differential expression (−0.1 to 0.1) were excluded from plotting. (C) LFC heatmap plot of all identified *P. marinus* DEGs in response to GDC-0152 pretreatment of hemocytes. (D) Bubble plot showing significantly enriched Biological Process and Molecular Function Gene Ontology terms identified by topGO in the DEGs.

BIRCs in un-supported groups, containing a novel Type Y BIR domain (LOC111100402) and the other with TII-DD-RING structure (LOC111100400) (annotations from Witkop et al., in press BMC Genomics). These results indicate that dual GDC-0152 and *P. marinus* treatment stimulated complex oxidation-reduction processes which may trigger or work alongside TNFR and NF-kB inflammatory pathways involved in regulating apoptosis, potentially leading to the increased suppression of apoptosis in this treatment. Results from the Z-VAD-FMK gene expression analysis are not presented here because no significant effect on apoptosis phenotype in dual challenge with *P. marinus* was found.

3.5. TNFR pathway and oxidoreductase transcripts were significantly associated with apoptosis inhibition in granulocytes following P. marinus and GDC-0152 treatment

WGCNA was performed to identify gene modules associated with further apoptosis suppression following dual GDC-0152 and *P. marinus* treatment. Forty-one modules were significantly correlated in the GDC-0152 and *P. marinus* treatment (Supplementary Figs. 6a and c). Specific modules were prioritized based on Module Membership (MM) and Gene Significance (GS) for apoptosis phenotype (arcsine transformed percentages of hemocytes that had engulfed *P. marinus* cells and were apoptotic), and if they had opposing directions of correlation for dual GDC-0152 and *P. marinus* treatment and apoptosis phenotype (Fig. 4a). Opposing directions of trait correlation were selected because transcripts potentially involved in apoptosis suppression in the dual GDC-0152 and *P. marinus* treatment group were hypothesized to be positively correlated with treatment (treatment leads to increased expression) and negatively correlated with apoptosis (treatment leads to decreased apoptosis).

This selection process identified the navajowhite2 module (264 total transcripts) as the most promising to investigate (Fig. 4b, c, d), and gene expression in this module was perfectly correlated ($r = 1$, $p = 7e\text{-}12$) with the hemocyte-only control *vs.* GDC-0152 and *P. marinus* treatment, highly negatively correlated with apoptosis phenotype ($r = -0.86$, $p = 3e\text{-}04$), and had a strong correlation between GS for apoptosis phenotype and MM (*cor* = 0.63), indicating genes strongly associated with apoptosis were also highly connected in this module (Fig. 4a and b). Enriched GO terms in this module overlapped with enriched terms in the differentially expressed transcripts from the dual GDC-0152 and *P. marinus* treatment, including protein binding, ion transport, and oxidoreductase activity (Fig. 4c). Two oxidoreductase-related transcripts were significantly correlated with apoptosis phenotype; 7-dehydrocholesterol reductase-like, transcript variant X2 (which was an intramodular hub gene, *i.e.* a highly interconnected gene with high trait significance), and cytochrome P450 2D27-like. Genes coding for cytochrome P450 enzymes, which play critical roles in ROS production (Zangar et al., 2004) were also differentially expressed in this treatment (13 cytochrome-related DEGs). This module also contained 79 intramodular hub genes strongly associated with apoptosis phenotype, 5 of which were apoptosis-related and differentially expressed in the DEG

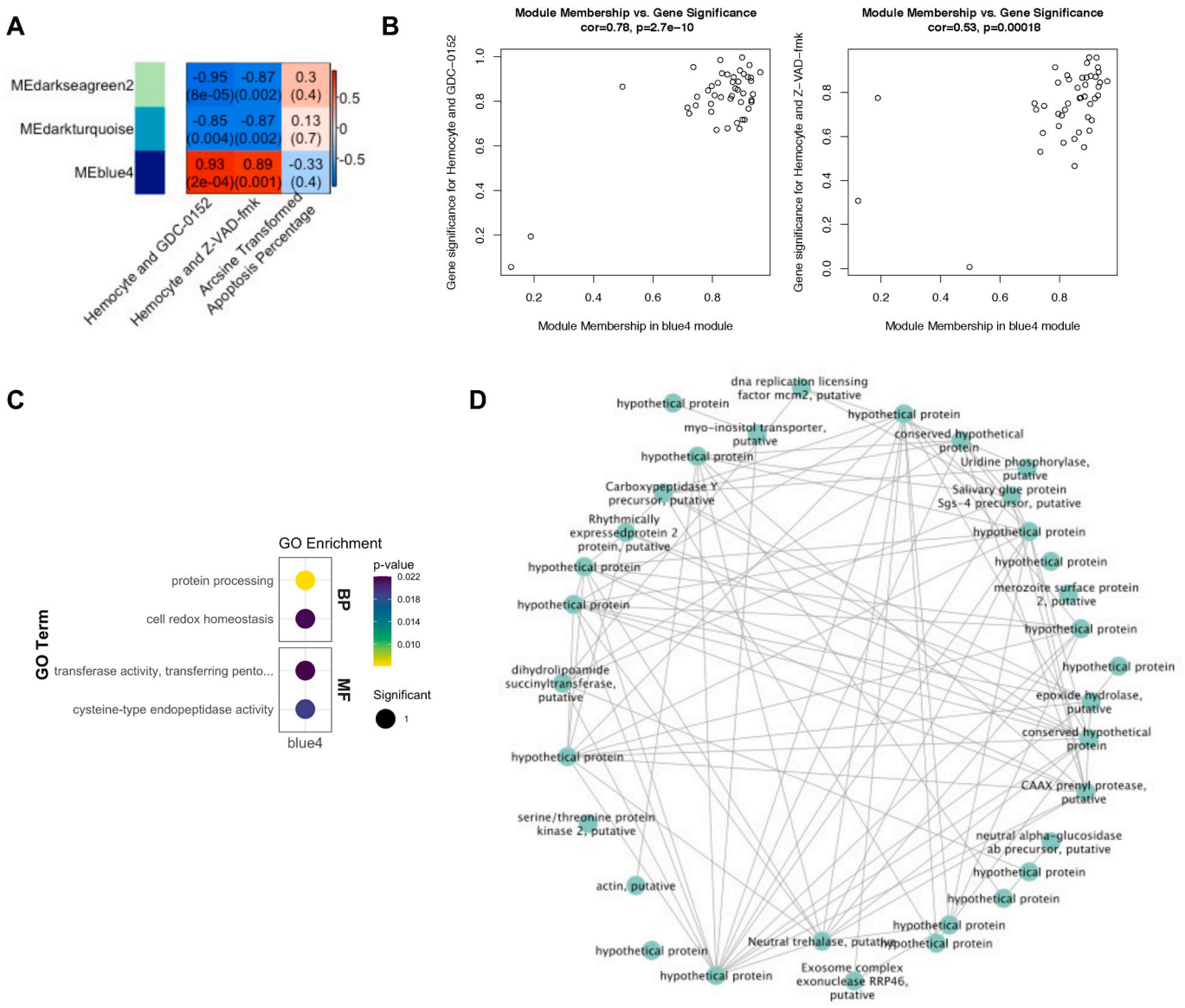

Fig. 6. WGCNA reveals correlation of *P. marinus* proteases, hydrolases, and kinases in response to hemocyte exposure. Hemocytes were pretreated with control (FSSW), 50 μM of GDC-0152 for 3 h, or 100 μM of Z-VAD-FMK for 1 h and then incubated with *P. marinus* (1:1 MOI) for 1 h before analysis of *P. marinus* gene expression. (A) Heatmap of modules significantly correlated with hemocyte and either GDC-0152 or Z-VAD-FMK treatment and high Gene Significance and Module Membership relationship in both treatments are plotted along with their correlation with apoptosis phenotype (percent of apoptosis in granulocytes). X-axis indicates modules of correlated transcripts and the y-axis plots each trait for which module significance was calculated. Correlation values (−1 to 1), followed by significance values (*p* between 0 and 1) in parentheses, are listed in each cell. Color indicates strength and direction of correlation. (B) Relationship between Gene Significance and Module Membership for the blue4 module, where each point is a transcript in the module. (C) Gene Ontology enrichment for Biological Process and Molecular Function for the blue4 module. (D) *P. marinus* blue4 module network (Cytoscape,V 3.8.0) showing highly connected intramodular hub genes. *P. marinus* modules were drawn using the circular layout.

analysis: caspase-2-like, heat shock protein 27-like, transcription factor AP-1-like, tumor necrosis factor receptor superfamily member 5-like, and the IAP uncharacterized LOC111100400, transcript variant X1 (a BIRC7-like protein; Witkop et al., in press BMC Genomics) (Fig. 4d). The module also contained a caspase-8-like and a cdc42 homolog transcript which were significantly correlated with apoptosis phenotype but not hub genes.

Overall, oxidoreductase and apoptosis-related transcripts in the module presented complex connection patterns (Fig. 4d). TNFR pathway transcripts (caspase 8-like, hsp-27-like, TNFRSF5-like) and inflammatory modulators (transcription factor AP-1, hsp-27) were directly connected with ROS production enzymes (cytochrome P450 2D27-like), suggesting they may work in similar pathways and/or may be co-regulated by GDC-0152 and *P. marinus* treatment. These results suggest GDC-0152 and *P. marinus* affect the NF-kB and TNFR pathways and oxidation-reduction processes in ways that are correlated with enhanced apoptosis suppression, providing further support that IAPs and NF-kB and TNFR pathways are important for apoptosis regulation in response to *P. marinus*.

3.6. *P. marinus* WGCNA identifies candidate proteases, hydrolases, and kinases for future study as potential NF-kB pathway or TNFR pathway modulators

Finally, *P. marinus* gene expression was contrasted in *P. marinus* incubated with GDC-0152 pretreated hemocytes or incubated with untreated hemocytes (*i.e.* effect of the IAP inhibition on *P. marinus* expression when co-incubated with hemocytes), to identify potential

parasite effectors that may be modulating/contributing to the hemocyte granulocyte apoptosis suppression observed in the IAP inhibitor – *P. marinus* treatment. *P. marinus* transformed expression data clustered by biological replicate and then by treatment (Fig. 5a), showing that pool identity (hemocyte context) had a stronger effect on *P. marinus* gene expression than the inhibitor treatment. Parasite differential gene expression in parasites that were incubated with the inhibitor pre-treated hemocytes as compared to non-treated hemocytes revealed 39 differentially expressed *P. marinus* transcripts, most of them upregulated (24 with LFCs >1 or < -1) (Fig. 5b and c). Unexpectedly, *P. marinus* DEG's did not include previously studied enzymes with known roles in *P. marinus* virulence and parasite apoptosis, such as superoxide dismutases and serine proteases (Joseph et al., 2010; Lau et al., 2018b; Xue, 2019), suggesting that IAP inhibitor treatment does not affect expression of these virulence factors (Supplementary Fig. 7). Transmembrane transporter activity and methyltransferase activity were among the few enriched GO terms in *P. marinus* in response to the IAP inhibitor (Fig. 5d). This result is consistent with general drug treatment response because increased expression of transporters, particularly ABC transporters, can play critical roles in drug resistance of protozoan parasites (Pramanik et al., 2019; Sauvage et al., 2009).

WGCNA analysis assessed correlation of *P. marinus* gene modules with treatment and apoptosis phenotype (measured as the level of apoptosis in granular hemocytes with engulfed *P. marinus*) (Fig. 6). To isolate modules of parasitic genes that may affect hemocyte apoptosis in general, and are not just responsive to hemocytes and a drug (*i.e.* inhibitor) treatment, modules of interest were those significantly correlated with both GDC-0152 and Z-VAD-FMK treatment and apoptosis phenotype. Only one module, blue4, was prioritized for analysis because it was positively correlated with both treatments and had a high correlation between Gene Significance and Module Membership, but no modules were significantly correlated with both *P. marinus* treatments and apoptosis phenotype (Fig. 6a, Supplementary Figs. 6b and d). Module blue4 contained 45 transcripts and was significantly enriched for protein processing, cell redox homeostasis, transferase activity, and cysteine-type endopeptidase activity GO terms (Fig. 6c). Of those enriched GO term-related transcripts, only one (CAAX prenyl protease, putative (XM_002772524.1, associated with cysteine-type endopeptidase activity) was a highly interconnected intramodular hub gene. The module also contained several other hub gene proteases, kinases, and hydrolases that could affect hemocyte apoptotic response; carboxypeptidase Y precursor, putative, containing serine carboxypeptidase domains (IPR001563), epoxide hydrolase, putative, containing hydrolytic enzyme domains (IPR000639, IPR000073), and serine/threonine protein kinase 2, putative, containing protein kinase domain profile (IPR000719) (Fig. 6d).

4. Discussion

This research investigated mechanisms underlying hemocyte apoptotic response to the protozoan parasite *P. marinus,* to identify molecular targets for modulation of host-parasite interactions in Dermo disease, a disease with a large economic and ecological impact on eastern oyster populations (Smolowitz, 2013). Because granulocytes, the major phagocytic immune cell of the oyster, may serve as a niche for *P. marinus*, prolonging the life of the granulocyte by decreasing granulocyte apoptosis may allow for enhanced parasite proliferation, dissemination through tissues, and disease (Hughes et al., 2010). Our results showed that basal apoptosis in unstimulated granulocytes may be IAP-dependent and involve caspase-independent pathways and confirmed that challenge of hemocytes with *P. marinus* for 1 h *in vitro* induced suppression of granulocyte apoptosis. Challenge with *P. marinus* alone triggered expression of oyster genes involved in catalytic and proteolytic activity, RNA binding, and metabolic processes in hemocytes, but few genes in apoptosis pathways, consistent with inhibition of apoptosis. Hemocyte pretreatment with the IAP inhibitor GDC-0152 revealed *P. marinus* may inhibit apoptosis downstream of membrane permeabilization, which could lead to upregulation of oxidation-reduction processes and modulation of TNFR and NF-kB pathway signaling and apoptosis inhibition. Finally, analysis of *P. marinus* gene expression using WGCNA identified candidate proteases, hydrolases, and kinases for future study as potential oyster NF-kB pathway or TNFR pathway modulators.

In vitro challenge of *C. virginica* hemocytes with *P. marinus* first revealed that *P. marinus* significantly suppressed granulocyte apoptosis, confirming previous studies (Goedken et al., 2005a; Hughes et al., 2010; Lau et al., 2018b). Despite the apoptosis suppression observed following hemocyte *P. marinus* challenge, few apoptosis pathway transcripts were significantly differentially expressed in response to *P. marinus*, which has been noted in previous studies in Dermo susceptible oysters (Prosestou and Sullivan, 2020). *P. marinus* challenge, on the other hand, did trigger expression of genes involved in catalytic activity, RNA binding, metabolic processes and serine-type endopeptidase inhibitor activity, which have been recognized as key components of eastern oyster defense against *P. marinus* (He et al., 2012; La Peyre et al., 2010; Xue, 2019; Xue et al., 2009; Yadavalli et al., 2020). The very limited apoptosis pathway differential expression response observed in hemocytes challenged with *P. marinus* (which notably involved a relatively higher proportion of the inhibitors of apoptosis IAPs as compared to other apoptosis molecules) indicates that interference of apoptosis pathways by *P. marinus* virulence factors may be an important mechanism of apoptosis suppression in hemocytes. Despite limitations in the experimental design in this research, in which lack of a *P. marinus* only control group prevented disentangling the effect of inhibitor pre-treatment of hemocytes on *P. marinus* gene expression from the effect of the hemocytes alone, several genes and pathways were expressed in *P. marinus* when incubated with hemocytes that may contribute to hemocyte apoptosis inhibition. These included transcripts involved in parasite cell-redox homeostasis, as well as proteases, hydrolases, and kinases. Further investigation would be required to confirm the potential role of these effectors potentially release by *P. marinus* on hemocyte apoptosis.

Treatment with the IAP inhibitor GDC-0152 alone caused a significant increase in granulocyte apoptosis, revealing that regulation of basal (unstimulated) hemocyte apoptosis in granulocytes may be IAP-dependent. A strong increase in apoptosis following GDC-0152 treatment has also been observed in other vertebrate and invertebrate species, and GDC-0152 is recognized as a potent apoptosis stimulator (Derakhshan et al., 2017; Erickson et al., 2013; Flygare et al., 2012; Hu et al., 2015; Rosner et al., 2019). Although treatment with GDC-0152 has been previously tested in urochordates (Rosner et al., 2019), this paper represents the first use of this novel, potent IAP inhibitor as an apoptosis modulator in molluscs. This research also provides the first functional evidence that IAPs are involved in apoptosis in oysters and supports that future work should be done to investigate their specific roles in apoptosis regulation.

Challenge with *P. marinus* following pre-treatment with the pan-caspase inhibitor Z-VAD-FMK suggested *P. marinus* suppresses apoptosis in hemocytes through inhibition of a caspase-independent pathway, because levels of apoptosis were not affected by treatment with this pan-caspase inhibitor. These results are consistent with previous research in which Z-VAD-FMK has been used to inhibit caspases in hemocytes challenged with *P. marinus* (Hughes et al., 2010). However, the effects of Z-VAD-FMK on caspase 3/7 inhibition were not strong in our research, and the inhibitor should be further tested at a range of concentrations to confirm this result. Caspase-independent apoptosis is typically triggered in physiological and pathological conditions in response to intrinsic stimuli following MOMP (Tait and Green, 2008). Triggering or modulation of caspase-independent apoptosis following intracellular infection has been observed previously in bacterial and parasite infections. For example, intracellular infection with *Mycobacterium bovis* triggers caspase-independent apoptosis by AIF and endoG

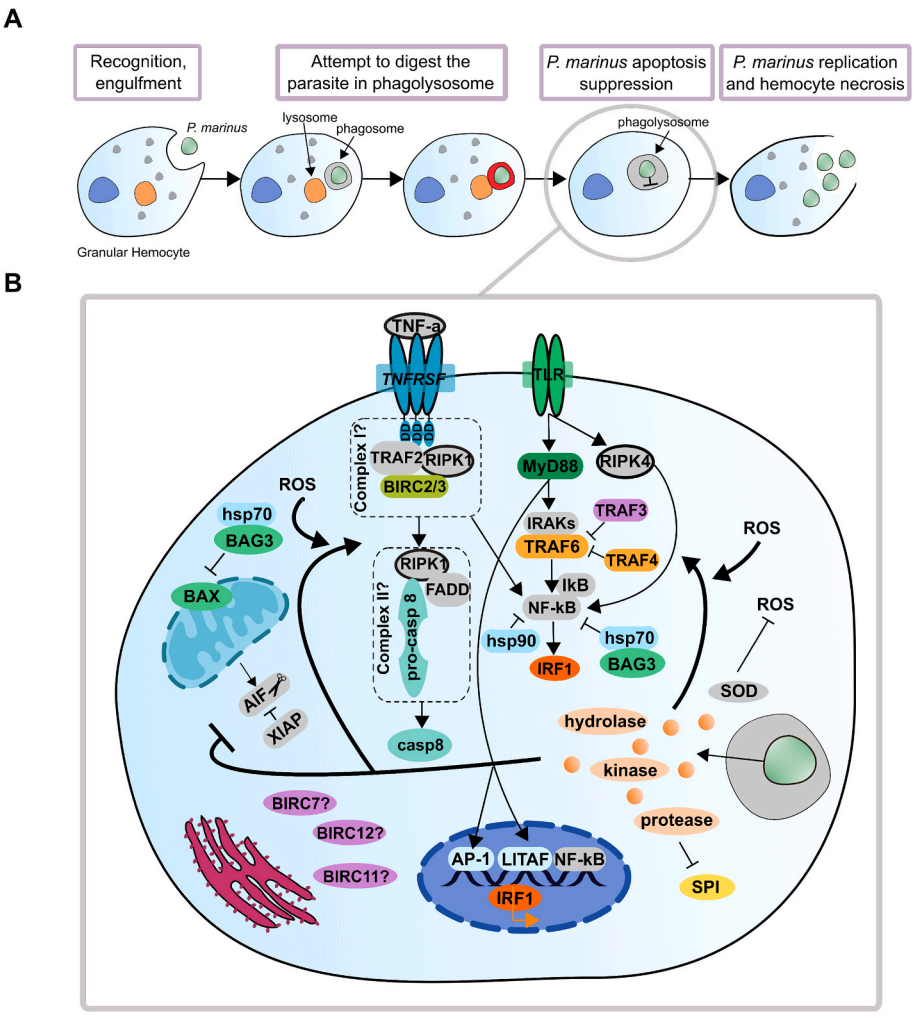

Fig. 7. *P. marinus*-induced hemocyte apoptosis suppression may involve interference with the TNFR or NF-kB pathways by *P. marinus* secreted enzymes and potential crosstalk with oxidation-reduction processes. (A) Model of *P. marinus* infection informed by this research and work in previous studies (Soudant et al., 2013; Tasumi and Vasta, 2007; Vasta et al., 2020). (B) Significantly differentially expressed genes and transcripts in eastern oyster hemocytes and *P. marinus* highlighted in this study were used to draw a hypothetical model of mechanism of action of *P. marinus* inhibition of eastern oyster hemocyte apoptosis. Critical molecules involved in implicated pathways but not significantly differentially expressed are outline in gray. Molecules involved in apoptosis pathways that have not been identified in eastern oysters (based on Witkop et al., in press BMC Genomics) are outlined in black.

(Benítez-Guzmán et al., 2018), host apoptosis following intracellular *Chlamydia* infection is caspase-independent (Perfettini et al., 2002), and *T. gondii* can block caspase-independent apoptosis in host cells through interference with granzyme B (Yamada et al., 2011). It is important to note, however, that although apoptosis observed here in eastern oyster hemocytes was potentially caspase-independent, oyster hemocyte apoptosis in other situations may be caspase-dependent (Romero et al., 2015). Overall, this finding is important for the study of hemocyte apoptotic response to *P. marinus* because it supports that other apoptosis enzymes, such as AIF (a critical caspase-independent apoptosis enzyme), may be involved in *P. marinus* apoptosis suppression.

Challenge with *P. marinus* following GDC-0152 pre-treatment revealed *P. marinus* was able to overcome the effects of GDC-0152 upon apoptosis stimulation, further suppressing apoptosis in hemocytes that had engulfed *P. marinus*. Interestingly, apoptosis suppression in the dual treatment of hemocytes with GDC-0152 and *P. marinus* was not accompanied by a decrease in mitochondrial outer membrane permeabilization (MOMP). These results suggest that *P. marinus* inhibits apoptosis downstream of MOMP, potentially through interference with an IAP-involved pathway or mechanism, such as interference with mitochondria-released apoptotic proteins such as AIF, which can be targeted for ubiquitination by BIRC4/XIAP – a target of GDC-0152 (Wilkinson et al., 2008). Intracellular parasite suppression of AIF is a known mechanism of apoptosis modulation, and *Toxoplasma gondii* can prevent the release of AIF following mitochondrial permeabilization (Mammari et al., 2019). Previous research in eastern oysters has shown that hemocyte apoptosis suppression 24 h post-*P. marinus* infection also led to significant upregulation of AIF gene expression (Lau et al., 2018b). In the flat oyster (*Ostrea edulis*), intracellular hemocyte infection with the protozoan parasite *Bonamia ostreae* induces early activation of hemocytes and upregulation of AIF expression, suggesting the involvement of AIF in intracellular infection (Gervais et al., 2018; Martín-Gómez et al., 2014). The differential gene expression analysis done in our research did not support, however, modulation of AIF or BIRC4 (XIAP), a key modulator of AIF, by *P. marinus*. This may be attributable to the short time frame of our challenge (1 h), and *P. marinus* modulation of AIF at longer time frames may be worth investigating, particularly in light of findings by Lau et al. (2018b) of greater AIF upregulation at 24 h post-challenge as compared to 6 h. Future inhibition or knockout assays should also be done to determine the role of AIF and BIRC4-like and other IAPs in the response of hemocytes exposed to *P. marinus*. These studies should additionally couple assays measuring MOMP with measurement of other intrinsic apoptosis markers, such as cytochrome *c* and AIF release from the mitochondria to help assess the full extent of MOMP, as MOMP can affect only a portion of a cell's mitochondria or be reversed (Ichim et al., 2015; Sun et al., 2017; Tang and Tang, 2018).

Alternatively, *P. marinus* may be targeting an IAP-involved pathway where MOMP does not necessarily occur (*i.e.* an extrinsic pathway as opposed to an intrinsic pathway) such as the TNFR pathway or NF-kB pathway where BIRC2/3 (cIAP1/2), another GDC-0152 target, are critical for signal transduction following extracellular ligand binding (Estornes and Bertrand, 2015). Although *P. marinus* challenge alone stimulated little apoptotic gene expression response in hemocytes, dual challenge with GDC-0152 and *P. marinus* stimulated TNFR and NF-kB

pathways and a much stronger oxidation-reduction response than *P. marinus* alone. GDC-0152 treatment in model systems induces NF-kB and TNF-α signaling (Erickson et al., 2013; Vasilikos et al., 2017). Likewise, ROS, which are important in oyster responses to *P. marinus* infection, have been shown to trigger the TNF-α and NF-kB pathway (Blaser et al., 2016; Morgan and Liu, 2011; Vazquez-Medina, 2017; Yang et al., 2020), and NF-kB and TNFR have been shown to be upregulated following *P. marinus* challenge in a previous report (Lau et al., 2018b). The correlation between TNFR pathway and oxidoreductase transcripts and further apoptosis suppression following GDC-0152 and *P. marinus* treatment, suggests there may be crosstalk between oxidation-reduction processes and the TNFR pathway, as observed in other studies (Blaser et al., 2016; Morgan and Liu, 2011; Yang et al., 2020). These results are also consistent with findings in other systems. For example, modulation of host cell survival through parasite-secreted enzymes, such as proteases and kinases, is key to host infection by *Toxoplasma gondii* and *Leishmania* spp. These parasite-secreted enzymes directly interfere with host NF-kB signaling pathways (Hodgson and Wan, 2016; Ihara and Nishikawa, 2021; Mammari et al., 2019; Sangaré et al., 2019b). The intracellular parasite *Cryptosporidium parvum* also can inhibit host cell apoptosis through activation of NF-kB (Di Genova and Tonelli, 2016; Mccole et al., 2000), and *T. gondii* dense granule protein GRA15 can activate the NF-kB pathway by interaction with TRAFs (Sangaré et al., 2019b). Similarly, flat oyster intracellular infection with the parasite *Bonamia ostreae* triggers TNF upregulation following challenge (Martín-Gómez et al., 2014). Future research should investigate the role of *P. marinus* proteases and enzymes identified here, as well as previously recognized proteases such as perkinsin (Faisal et al., 1999; Xue et al., 2006), in NF-kB and TNFR pathway modulation in hemocytes.

5. Conclusion

Through a combination of phenotypic assays, treatment with chemical inhibitors of apoptosis pathway proteins (caspases and IAPs), and dual transcriptomic analysis of *C. virginica* and *P. marinus*, we conclude that: (1) basal hemocyte apoptosis in *C. virginica* may be IAP-dependent, (2) *P. marinus* apoptosis suppression may involve caspase-independent apoptosis pathways, and (3) apoptosis suppression by the parasite likely occurs downstream or independently of mitochondrial permeabilization. The discovery that hemocyte apoptosis may be IAP-dependent is a novel finding that highlights the need for future work to determine the functions of members of this expanded and diverse gene family (annotated in Witkop et al., in press BMC Genomics). This research also indicates that (4) the mechanism of *P. marinus* apoptosis suppression in hemocytes involves oxidation-reduction processes and TNFR and NF-kB pathway modulation in hemocytes. Synthesis of the phenotype and gene expression evidence presented here, combined with knowledge from previous research (Fernández-Robledo et al., 2008; Lau et al., 2018b; Smolowitz, 2013; Soudant et al., 2013), suggests a new, hypothetical model for mechanisms of apoptosis suppression in eastern oyster hemocytes following *P. marinus* intracellular infection (Fig. 7). Following engulfment of *P. marinus*, hemocytes generate ROS and express serine protease inhibitors, while *P. marinus* secretes enzymes such as proteases, hydrolases, and kinases that activate the TNFR and NF-kB pathways, promoting cell survival, and/or interfere with mitochondrial secreted caspase-independent apoptosis enzymes such as AIF, resulting in suppression of apoptosis downstream of mitochondrial membrane permeabilization in a caspase-independent manner. These pathways may also involve crosstalk between ROS and the NF-kB and TNFR pathways (Morgan and Liu, 2011; Vazquez-Medina, 2017). Overall, this study informs future research of *P. marinus* apoptosis suppression mechanisms in the eastern oyster, advancing our general understanding of apoptosis in invertebrate host-parasite interactions.

Funding

This work was supported by a USDA NIFA Pre-Doctoral Fellowship Award# 2019-67011-29553 to EMW, USDA NIFA AFRI Award #2015-67016-22942 to MGC and Wesley Warren, USDA ARS Collaborative Project 58-8030-5-009 to MGC, a USDA NRSP-8 award to MGC and DAP, and the Blount Family Narragansett Bay Shellfish Restoration Foundation.

Declaration of competing interest

None.

Acknowledgements

The authors thank Stan Allen and Jessica Small at VIMS ABC for supplying lines of selectively bred oysters. The authors thank the NOAA Northeast Fisheries Science Center Milford Laboratory for authorized use of their BD Accuri C6+ flow cytometer, and Shannon Meseck at NOAA for assistance with flow cytometer troubleshooting. The authors also acknowledge Margaret Schedl (URI) for assistance performing the flow cytometry and transcriptome experiment.

Appendix A. Supplementary data

Supplementary data to this article can be found online at https://doi.org/10.1016/j.dci.2022.104339.

References

Alavi, M.R., Fernández-Robledo, J., Vasta, G.R., 2009. Development of an in vitro assay to examine intracellular survival of Perkinsus marinus trophozoites upon phagocytosis by oyster (Crassostrea virginica and Crassostrea ariakensis) hemocytes. J. Parasitol. 95, 900–907. https://doi.org/10.1645/GE-1864.1.

Alexa, A., Rahnenfuhrer, J., 2019. topGO: Enrichment Analysis for Gene Ontology. R Studio package v 2.36.0.

Allam, B., Carden, W.E., Ward, J.E., Ralph, G., Winnicki, S., Pales Espinosa, E., 2013. Early host-pathogen interactions in marine bivalves: evidence that the alveolate parasite Perkinsus marinus infects through the oyster mantle during rejection of pseudofeces. J. Invertebr. Pathol. 113, 26–34. https://doi.org/10.1016/j.jip.2012.12.011.

Anderson, R.S., 1999. Perkinsus marinus secretory products modulate superoxide anion production by oyster (Crassostrea virginica) haemocytes. Fish Shellfish Immunol. 9, 51–60. https://doi.org/10.1006/fsim.1998.0174.

Anderson, R.S., Paynter, K.T., Burreson, E.M., 1992. Increased reactive oxygen intermediate production by hemocytes withdrawn from Crassostrea virginica infected with Perkinsus marinus. Ref. Biol. Bull 183. https://doi.org/10.2307/1542024, 476–48.

Benítez-Guzmán, A., Arriaga-Pizano, L., Morán, J., Gutiérrez-Pabello, J.A., 2018. Endonuclease G takes part in AIF-mediated caspase-independent apoptosis in Mycobacterium bovis-infected bovine macrophages. Vet. Res. 49, 1–9. https://doi.org/10.1186/s13567-018-0567-1.

Blaser, H., Dostert, C., Mak, T.W., Brenner, D., 2016. TNF and ROS crosstalk in inflammation. Trends Cell Biol. 26, 249–261. https://doi.org/10.1016/j.tcb.2015.12.002.

Bushek, D., Allen, S.K., 1996. Host-parasite interactions among broadly distributed populations of the eastern oyster Crassostrea virginica and the protozoan Perkinsus marinus. Mar. Ecol. Prog. Ser. 139, 127–141. https://doi.org/10.3354/meps139127.

Bushnell, B., 2014. BBMap: A Fast, Accurate, Splice-Aware Aligner. Accessed through https://sourceforge.net/projects/bbmap/.

Chakraborti, S., Chakraborti, T., Chattopadhyay, D., Shaha, C., 2019. Oxidative stress in microbial diseases, oxidative stress in microbial diseases. Springer, Singapore. https://doi.org/10.1007/978-981-13-8763-0.

Croxton, A.N., Wikfors, G.H., Schulterbrandt-Gragg, R.D., 2012. Immunomodulation in eastern oysters, Crassostrea virginica, exposed to a PAH-contaminated, microphytobenthic diatom. Aquat. Toxicol. 118–119, 27–36. https://doi.org/10.1016/j.aquatox.2012.02.023.

Dean, P., Major, P., Nakjang, S., Hirt, R.P., Martin Embley, T., 2014. Transport proteins of parasitic protists and their role in nutrient salvage. Front. Plant Sci. 5 https://doi.org/10.3389/fpls.2014.00153.

Derakhshan, A., Chen, Z., Van Waes, C., 2017. Therapeutic small molecules target inhibitor of apoptosis proteins in cancers with deregulation of extrinsic and intrinsic cell death pathways. Clin. Cancer Res. 23, 1379–1387. https://doi.org/10.1158/1078-0432.CCR-16-2172.

Di Genova, B.M., Tonelli, R.R., 2016. Infection strategies of intestinal parasite pathogens and host cell responses. Front. Microbiol. 7, 1–16. https://doi.org/10.3389/fmicb.2016.00256.

Ekert, P.G., Silke, J., Vaux, D.L., 1999. Caspase inhibitors. Cell Death Differ. 6, 1081–1086. https://doi.org/10.1038/sj.cdd.4400594.
Erickson, R.I., Tarrant, J., Cain, G., Lewin-Koh, S.C., Dybdal, N., Wong, H., Blackwood, E., West, K., Steigerwalt, R., Mamounas, M., Flygare, J.A., Amemiya, K., Dambach, D., Fairbrother, W.J., Diaz, D., 2013. Toxicity profile of small-molecule IAP antagonist GDC-0152 is linked to TNF-α pharmacology. Toxicol. Sci. 131, 247–258. https://doi.org/10.1093/toxsci/kfs265.
Estornes, Y., Bertrand, M.J.M., 2015. IAPs, regulators of innate immunity and inflammation. Semin. Cell Dev. Biol. 39, 106–114. https://doi.org/10.1016/j.semcdb.2014.03.035.
Faisal, M., Schafhauser, D.Y., Garreis, K.A., Elsayed, E., La Peyre, J.F., 1999. Isolation and characterization of Perkinsus marinus proteases using bacitracin-sepharose affinity chromatography. Comp. Biochem. Physiol. B Biochem. Mol. Biol. 123, 417–426. https://doi.org/10.1016/S0305-0491(99)00088-7.
Fernández-Robledo, J.A., Schott, E.J., Vasta, G.R., 2008. Perkinsus marinus superoxide dismutase 2 (PmSOD2) localizes to single-membrane subcellular compartments. Biochem. Biophys. Res. Commun. 375, 215–219. https://doi.org/10.1016/j.bbrc.2008.07.162.
Flygare, J.A., Beresini, M., Budha, N., Chan, H., Chan, I.T., Cheeti, S., Cohen, F., Deshayes, K., Doerner, K., Eckhardt, S.G., Elliott, L.O., Feng, B., Franklin, M.C., Reisner, S.F., Gazzard, L., Halladay, J., Hymowitz, S.G., La, H., LoRusso, P., Maurer, B., Murray, L., Plise, E., Quan, C., Stephan, J.-P., Young, S.G., Tom, J., Tsui, V., Um, J., Varfolomeev, E., Vucic, D., Wagner, A.J., Wallweber, H.J.A., Wang, L., Ware, J., Wen, Z., Wong, H., Wong, J.M., Wong, M., Wong, S., Yu, R., Zobel, K., Fairbrother, W.J., 2012. Discovery of a potent small-molecule antagonist of inhibitor of apoptosis (IAP) proteins and clinical candidate for the treatment of cancer (GDC-0152). J. Med. Chem. 55, 4101–4113. https://doi.org/10.1021/jm300060k.
Ford, S.E., Chintala, M.M., Bushek, D., 2002. Comparison of in vitro-cultured and wild-type Perkinsus marinus. I. pathogen virulence. Dis. Aquat. Org. 51, 187–201. https://doi.org/10.3354/dao051187.
Galluzzi, L., López-Soto, A., Kumar, S., Kroemer, G., 2016. Caspases connect cell-death signaling to organismal homeostasis. Immunity 44, 221–231. https://doi.org/10.1016/j.immuni.2016.01.020.
Gerdol, M., Gomez-Chiarri, M., Castillo, M.G., Figueras, A., et al., 2018. Immunity in molluscs: recognition and effector mechanisms, with a focus on Bivalvia. In: Cooper, E. (Ed.), Advances in Comparative Immunology. Springer International Publishing, pp. 225–341.
Gervais, O., Renault, T., Arzul, I., 2018. Molecular and cellular characterization of apoptosis in flat oyster a key mechanisms at the heart of host-parasite interactions. Sci. Rep. 8, 1–12. https://doi.org/10.1038/s41598-018-29776-x.
Goedken, M., Morsey, B., Sunila, I., De Guise, S., 2005a. Immunomodulation of Crassostrea gigas and Crassostrea virginica cellular defense mechanism by Perkinsus marinus. J. Shellfish Res. 24, 487–496. https://doi.org/10.2983/0730-8000, 2005) 24.
Goedken, M., Morsey, B., Sunila, I., Dungan, C., De Guise, S., 2005b. The effects of temperature and salinity on apoptosis of Crassostrea virginica hemocytes and Perkinsus marinus. J. Shellfish Res. 24, 177–183.
Gu, Z., Eils, R., Schlesner, M., 2016. Complex heatmaps reveal patterns and correlations in multidimensional genomic data. Bioinformatics 32, 2847–2849. https://doi.org/10.1093/bioinformatics/btw313.
He, Y., Yu, H., Bao, Z., Zhang, Q., Guo, X., 2012. Mutation in promoter region of a serine protease inhibitor confers Perkinsus marinus resistance in the eastern oyster (Crassostrea virginica). Fish Shellfish Immunol. 33, 411–417. https://doi.org/10.1016/j.fsi.2012.05.028.
Hégaret, H., Wikfors, G.H., Soudant, P., 2003a. Flow cytometric analysis of haemocytes from eastern oysters, Crassostrea virginica, subjected to a sudden temperature elevation II. Haemocyte functions: aggregation, viability, phagocytosis, and respiratory burst. J. Exp. Mar. Biol. Ecol. 293, 249–265. https://doi.org/10.1016/S0022-0981(03)00235-1.
Hégaret, H., Wikfors, G.H., Soudant, P., 2003b. Flow-cytometric analysis of haemocytes from eastern oysters, Crassostrea virginica, subjected to a sudden temperature elevation I. Haemocyte types and morphology. J. Exp. Mar. Biol. Ecol. 293, 237–248. https://doi.org/10.1016/S0022-0981(03)00236-3.
Hodgson, A., Wan, F., 2016. Interference with nuclear factor kappaB signaling pathway by pathogen-encoded proteases: global and selective inhibition. Mol. Microbiol. 99, 439–452. https://doi.org/10.1111/mmi.13245.
Hu, R., Li, J., Liu, Z., Miao, M., Yao, K., 2015. GDC-0152 induces apoptosis through down-regulation of IAPs in human leukemia cells and inhibition of PI3K/Akt signaling pathway. Tumor Biol. 36, 577–584. https://doi.org/10.1007/s13277-014-2648-8.
Hughes, F.M., Foster, B., Grewal, S., Sokolova, I.M., 2010. Apoptosis as a host defense mechanism in Crassostrea virginica and its modulation by Perkinsus marinus. Fish Shellfish Immunol. 29, 247–257. https://doi.org/10.1016/j.fsi.2010.03.003.
Ichim, G., Lopez, J., Ahmed, S.U., Muthalagu, N., Giampazolias, E., Delgado, M.E., Haller, M., Riley, J.S., Mason, S.M., Athineos, D., Parsons, M.J., vandeKooij, B., Bouchier-Hayes, L., Chalmers, A.J., Rooswinkel, R.W., Oberst, A., Blyth, K., Rehm, M., Murphy, D.J., Tait, S.W.G., 2015. Limited mitochondrial permeabilization causes DNA damage and genomic instability in the absence of cell death. Mol. Cell. 57, 860–872. https://doi.org/10.1016/j.molcel.2015.01.018.
Ihara, F., Nishikawa, Y., 2021. Toxoplasma gondii manipulates host cell signaling pathways via its secreted effector molecules. Parasitol. Int. 83, 102368. https://doi.org/10.1016/j.parint.2021.102368.
Joseph, S.J., Fernández-Robledo, J.A., Gardner, M.J., El-Sayed, N.M., Kuo, C.H., Schott, E.J., Wang, H., Kissinger, J.C., Vasta, G.R., 2010. The alveolate Perkinsus marinus: biological insights from EST gene discovery. BMC Genom. 11 https://doi.org/10.1186/1471-2164-11-228.
Kim, D., Langmead, B., Salzberg, S.L., 2016. HISAT: a fast spliced aligner with low memory requirements. Daehwan 12, 357–360. https://doi.org/10.1038/nmeth.3317.
Kiss, T., 2010. Apoptosis and its functional significance in molluscs. Apoptosis 15, 313–321. https://doi.org/10.1007/s10495-009-0446-3.
La Peyre, J.F., Chu, F. lin E., Vogelbein, W.K., 1995. In vitro interaction of Perkinsus marinus merozoites with eastern and pacific oyster hemocytes. Dev. Comp. Immunol. 19, 291–304. https://doi.org/10.1016/0145-305X(95)00017-N.
La Peyre, J.F., Xue, Q.G., Itoh, N., Li, Y., Cooper, R.K., 2010. Serine protease inhibitor cvSI-1 potential role in the eastern oyster host defense against the protozoan parasite Perkinsus marinus. Dev. Comp. Immunol. 34, 84–92. https://doi.org/10.1016/j.dci.2009.08.007.
Langfelder, P., Horvath, S., 2008. WGCNA: an R package for weighted correlation network analysis. BMC Bioinf. 9 https://doi.org/10.1186/1471-2105-9-559.
Langfelder, P., Luo, R., Oldham, M.C., Horvath, S., 2011. Is my network module preserved and reproducible? PLoS Comput. Biol. 7 https://doi.org/10.1371/journal.pcbi.1001057.
Lau, Y.T., Gambino, L., Santos, B., Pales Espinosa, E., Allam, B., 2018a. Regulation of oyster (Crassostrea virginica) hemocyte motility by the intracellular parasite Perkinsus marinus : a possible mechanism for host infection. Fish Shellfish Immunol. https://doi.org/10.1016/j.fsi.2018.04.019.
Lau, Y.T., Santos, B., Barbosa, M., Pales Espinosa, E., Allam, B., 2018b. Regulation of apoptosis-related genes during interactions between oyster hemocytes and the alveolate parasite Perkinsus marinus. Fish Shellfish Immunol. 83, 180–189. https://doi.org/10.1016/j.fsi.2018.09.006.
Li, H., Handsaker, B., Wysoker, A., Fennell, T., Ruan, J., Homer, N., Marth, G., Abecasis, G., Durbin, R., 2009. The sequence alignment/map format and SAMtools. Bioinformatics 25, 2078–2079. https://doi.org/10.1093/bioinformatics/btp352.
Liu, Y., Gu, H.Y., Zhu, J., Niu, Y.M., Zhang, C., Guo, G.L., 2019. Identification of hub genes and key pathways associated with bipolar disorder based on weighted gene Co-expression network analysis. Front. Physiol. 10, 1–9. https://doi.org/10.3389/fphys.2019.01081.
Lodoen, M.B., Lima, T.S., 2019. Mechanisms of human innate immune evasion by Toxoplasma gondii. Front. Cell. Infect. Microbiol. 9, 103. https://doi.org/10.3389/fcimb.2019.00103.
Love, M.I., Huber, W., Anders, S., 2014. Moderated estimation of fold change and dispersion for RNA-seq data with DESeq2. Genome Biol. 15, 1–21. https://doi.org/10.1186/s13059-014-0550-8.
Mammari, N., Halabi, M.A., Yaacoub, S., Chlala, H., Dardé, M.-L., Courtioux, B., 2019. Toxoplasma gondii modulates the host cell responses: an overview of apoptosis pathways. BioMed Res. Int. https://doi.org/10.1155/2019/6152489, 2019.
Martín-Gómez, L., Villalba, A., Carballal, M.J., Abollo, E., 2014. Molecular characterisation of TNF, AIF, dermatopontin and VAMP genes of the flat oyster Ostrea edulis and analysis of their modulation by diseases. Gene 533, 208–217. https://doi.org/10.1016/j.gene.2013.09.085.
Mccole, D.F., Eckmann, L., Laurent, F., Kagnoff, M.F., 2000. Intestinal epithelial cell apoptosis following Cryptosporidium parrum infection. Infect. Immun. 68, 1710–1713. https://doi.org/10.1128/IAI.68.3.1710-1713.2000.
Morgan, M.J., Liu, Z.G., 2011. Crosstalk of reactive oxygen species and NF-κB signaling. Cell Res. 21, 103–115. https://doi.org/10.1038/cr.2010.178.
Perfettini, J.L., Reed, J.C., Israël, N., Martinou, J.C., Dautry-Varsat, A., Ojcius, D.M., 2002. Role of Bcl-2 family members in caspase-independent apoptosis during Chlamydia infection. Infect. Immun. 70, 55–61. https://doi.org/10.1128/IAI.70.1.55-61.2002.
Pertea, M., Kim, D., Pertea, G.M., Leek, J.T., Salzberg, S.L., 2016. Transcript-level expression analysis of RNA- seq experiments with HISAT , StringTie and Transcript-level expression analysis of RNA-seq experiments with HISAT , StringTie and Ballgown. Nat. Protoc. 11, 1650–1667. https://doi.org/10.1038/nprot.2016-095.
Pramanik, P.K., Alam, M.N., Roy Chowdhury, D., Chakraborti, T., 2019. Drug resistance in Protozoan parasites: an incessant wrestle for survival. J. Glob. Antimicrob. Resist. 18, 1–11. https://doi.org/10.1016/j.jgar.2019.01.023.
Proestou, D.A., Sullivan, M.E., 2020. Variation in global transcriptomic response to Perkinsus marinus infection among eastern oyster families highlights potential mechanisms of disease resistance. Fish Shellfish Immunol. 96, 141–151. https://doi.org/10.1016/j.fsi.2019.12.001.
Proestou, D.A., Corbett, R.J., Ben-Horin, T., Small, J.M., Allen Jr., S.K., 2019. Defining Dermo resistance phenotypes in an eastern oyster breeding population. Aquacult. Res. 50, 2142–2154. https://doi.org/10.1111/are.14095.
R Studio Team, 2020. RStudio: Integrated Development for R. R Studio, Boston, MA. http://www.rstudio.com.
Rodriguez, C., Simon, V., Conget, P., Vega, I.A., 2020. Both quiescent and proliferating cells circulate in the blood of the invasive apple snail Pomacea canaliculata. Fish Shellfish Immunol. 107, 95–103. https://doi.org/10.1016/j.fsi.2020.09.026.
Romero, A., Novoa, B., Figueras, A., 2015. The complexity of apoptotic cell death in mollusks: an update. Fish Shellfish Immunol. 46, 79–87. https://doi.org/10.1016/j.fsi.2015.03.038.
Rosner, A., Kravchenko, O., Rinkevich, B., 2019. IAP genes partake weighty roles in the astogeny and whole body regeneration in the colonial urochordate Botryllus schlosseri. Dev. Biol. 448, 320–341. https://doi.org/10.1016/j.ydbio.2018.10.015.
Sangaré, L.O., Yang, N., Konstantinou, E.K., Lu, D., Mukhopadhyay, D., Young, L.H., Saeij, J.P.J., 2019a. Toxoplasma GRA15 activates the NF-Kb pathway through interactions with TNF receptor-associated factors. mBio 10, 1–13. https://doi.org/10.1128/mbio.00808-19.

Sangaré, L.O., Yang, N., Konstantinou, E.K., Lu, D., Mukhopadhyay, D., Young, L.H., Saeij, J.P.J., 2019b. Toxoplasma GRA15 activates the NF-Kb pathway through interactions with TNF receptor-associated factors. mBio 10, 1–13. https://doi.org/10.1128/mbio.00808-19.

Sauvage, V., Aubert, D., Escotte-Binet, S., Villena, I., 2009. The role of ATP-binding cassette (ABC) proteins in protozoan parasites. Mol. Biochem. Parasitol. 167, 81–94. https://doi.org/10.1016/j.molbiopara.2009.05.005.

Schott, E.J., Pecher, W.T., Okafor, F., Vasta, G.R., 2003. The protistan parasite Perkinsus marinus is resistant to selected reactive oxygen species. Exp. Parasitol. 105, 232–240. https://doi.org/10.1016/j.exppara.2003.12.012.

Shannon, P., Markiel, A., Ozier, O., Baliga, N.S., Wang, J.T., Ramage, D., Amin, N., Schwikowski, B., Ideker, T., 2003. Cytoscape: a software environment for integrated models of biomolecular interaction networks. Genome Res. 13, 2498–2504. https://doi.org/10.1101/gr.1239303.

Siqueira-Neto, J.L., Debnath, A., McCall, L.I., Bernatchez, J.A., Ndao, M., Reed, S.L., Rosenthal, P.J., 2018. Cysteine proteases in protozoan parasites. PLoS Neglected Trop. Dis. 12, 1–20. https://doi.org/10.1371/journal.pntd.0006512.

Smolowitz, R., 2013. A review of current state of knowledge concerning Perkinsus marinus effects on Crassostrea virginica (Gmelin) (the Eastern Oyster), 50, pp. 404–411. https://doi.org/10.1177/0300985813480806.

Soudant, P., Chu, F.E., Volety, A., 2013. Host – parasite interactions : marine bivalve molluscs and protozoan parasites , Perkinsus species. J. Invertebr. Pathol. 114, 196–216. https://doi.org/10.1016/j.jip.2013.06.001.

Sullivan, M.E., Proestou, D.A., 2021. Survival and transcriptomic responses to different Perkinsus marinus exposure methods in an Eastern oyster family. Aquaculture 542, 736831. https://doi.org/10.1016/j.aquaculture.2021.736831.

Sun, G., Guzman, E., Zhou, H.R., Kosik, K.S., Montell, D.J., 2017. A molecular signature for anastasis, recovery from the brink of apoptotic cell death. bioRxiv 216, 3355–3368. https://doi.org/10.1101/102640.

Supek, F., Bošnjak, M., Škunca, N., Šmuc, T., 2011. Revigo summarizes and visualizes long lists of gene ontology terms. PLoS One 6. https://doi.org/10.1371/journal.pone.0021800.

Tait, S.W.G., Green, D.R., 2008. Caspase-independent cell death: leaving the set without the final cut. Oncogene 27, 6452–6461. https://doi.org/10.1038/onc.2008.311.

Tang, H.M., Tang, H.L., 2018. Anastasis: recovery from the brink of cell death. R. Soc. Open Sci. 5 https://doi.org/10.1098/rsos.180442.

Tasumi, S., Vasta, G.R., 2007. A galectin of unique domain organization from hemocytes of the eastern oyster (Crassostrea virginica) is a receptor for the protistan parasite Perkinsus marinus. J. Immunol. 179, 3086–3098. https://doi.org/10.4049/jimmunol.179.5.3086.

Tchoghandjian, A., Soubéran, A., Tabouret, E., Colin, C., Denicolaï, E., Jiguet-Jiglaire, C., El-Battari, A., Villard, C., Baeza-Kallee, N., Figarella-Branger, D., 2016. Inhibitor of apoptosis protein expression in glioblastomas and their in vitro and in vivo targeting by SMAC mimetic GDC-0152. Cell Death Dis. 7, 1–10. https://doi.org/10.1038/cddis.2016.214.

Vasilikos, L., Spilgies, L.M., Knop, J., Wong, W.W.L., 2017. Regulating the balance between necroptosis, apoptosis and inflammation by inhibitors of apoptosis proteins. Immunol. Cell Biol. 95, 160–165. https://doi.org/10.1038/icb.2016.118.

Vasta, G.R., Wang, J., 2020. Galectin-mediated immune recognition: opsonic roles with contrasting outcomes in selected shrimp and bivalve mollusk species. Dev. Comp. Immunol. https://doi.org/10.1016/j.dci.2020.103721, 103721.

Vasta, G.R., Feng, C., Tasumi, S., Abernathy, K., Bianchet, M.A., Wilson, I.B.H., Paschinger, K., Wang, L.X., Iqbal, M., Ghosh, A., Amin, M.N., Smith, B., Brown, S., Vista, A., 2020. Biochemical characterization of oyster and clam galectins: selective recognition of carbohydrate ligands on host hemocytes and Perkinsus parasites. Front. Chem. 8, 1–15. https://doi.org/10.3389/fchem.2020.00098.

Vazquez-Medina, J.P., 2017. Redox Signaling and the Onset of the Inflammatory Cascade, Immunity and Inflammation in Health and Disease: Emerging Roles of Nutraceuticals and Functional Foods in Immune Support. Elsevier Inc. https://doi.org/10.1016/B978-0-12-805417-8.00003-2.

Volety, A.K., Chu, F.L.E., 1995. Suppression of chemiluminescence of eastern oyster (*Crassostrea virginica*) hemocytes by the protozoan parasite Perkinsus marinus. Dev. Comp. Immunol. 19, 135–142. https://doi.org/10.1016/0145-305X(94)00059-O.

Wikfors, G.H., Alix, J.H., 2014. Granular hemocytes are phagocytic, but agranular hemocytes are not, in the Eastern Oyster Crassostrea virginica. Invertebr. Immun. 1, 15–21. https://doi.org/10.2478/invim-2014-0001.

Wilkinson, J.C., Wilkinson, A.S., Galbán, S., Csomos, R.A., Duckett, C.S., 2008. Apoptosis-inducing factor is a target for ubiquitination through interaction with XIAP. Mol. Cell Biol. 28, 237–247. https://doi.org/10.1128/mcb.01065-07.

Witkop, E.M., Proestou, D.A., Gómez-Chiarri, M., n.d. The expanded Inhibitor of Apoptosis gene family in oysters possesses novel domain architectures and may play diverse roles in apoptosis following immune challenge. Press. BMC Genom..

Xue, Q., 2019. Pathogen proteases and host protease inhibitors in molluscan infectious diseases. J. Invertebr. Pathol. 166, 107214. https://doi.org/10.1016/j.jip.2019.107214.

Xue, Q.G., Waldrop, G.L., Schey, K.L., Itoh, N., Ogawa, M., Cooper, R.K., Losso, J.N., La Peyre, J.F., 2006. A novel slow-tight binding serine protease inhibitor from eastern oyster (*Crassostrea virginica*) plasma inhibits perkinsin, the major extracellular protease of the oyster protozoan parasite *Perkinsus marinus*. Comp. Biochem. Physiol. B Biochem. Mol. Biol. 145, 16–26. https://doi.org/10.1016/j.cbpb.2006.05.010.

Xue, Q., Itoh, N., Schey, K.L., Cooper, R.K., La Peyre, J.F., 2009. Evidence indicating the existence of a novel family of serine protease inhibitors that may be involved in marine invertebrate immunity. Fish Shellfish Immunol. 27, 250–259. https://doi.org/10.1016/j.fsi.2009.05.006.

Yadavalli, R., Umeda, K., Fernández Robledo, J.A., 2020. *Perkinsus marinus*. Trends Parasitol. 36 (12), 1013–1014. https://doi.org/10.1016/j.pt.2020.05.002.

Yamada, T., Tomita, T., Weiss, L.M., Orlofsky, A., 2011. Toxoplasma gondii inhibits granzyme B-mediated apoptosis by the inhibition of granzyme B function in host cells. Int. J. Parasitol. 41, 595–607. https://doi.org/10.1016/j.ijpara.2010.11.012.

Yang, Z., Min, Z., Yu, B., 2020. Reactive oxygen species and immune regulation. Int. Rev. Immunol. 39, 292–298. https://doi.org/10.1080/08830185.2020.1768251.

Yee, A., Dungan, C., Hamilton, R., Goedken, M., Guise, S.D.E., Sunila, I., 2005. Apoptosis of the protozoan oyster pathogen Perkinsus marinus in vivo and in vitro in the Chesapeake Bay and the long island sound. J. Shellfish Res. 24, 1035–1042. https://doi.org/10.2983/0730-8000, 2005)24[1035:aotpop]2.0.co;2.

Zangar, R.C., Davydov, D.R., Verma, S., 2004. Mechanisms that regulate production of reactive oxygen species by cytochrome P450. Toxicol. Appl. Pharmacol. 199, 316–331. https://doi.org/10.1016/j.taap.2004.01.018.

Zhu, A., Ibrahim, J.G., Love, M.I., 2018. Heavy-tailed prior distributions for sequence count data: removing the noise and preserving large differences. Bioinformatics 35, 2084–2092. https://doi.org/10.1093/bioinformatics/bty895.